Construction and Building Materials 538 (2026) 147142

Contents lists available at ScienceDirect

Construction and Building Materials

journal homepage: www.elsevier.com/locate/conbuildmat

Stiffness and strength of beech, birch and spruce in compression perpendicular to the grain and rolling shear: Influence of moisture content, annual ring structure, and test method

Eva Binder [a,b,*], Elisabet Kuck [c], Christian Bertram [c], Zijad Shehadeh [a,b], Michael Schweigler [a,b], Carmen Sandhaas [c], Thomas K. Bader [a,b]

[a] Department of Building Technology, Linnaeus University, Universitetsplatsen 1, Växjö, 35195, Sweden
[b] Linnaeus University Centre for Competitive Timber Structures, Linnaeus University, Universitetsplatsen 1, Växjö, 35195, Sweden
[c] KIT Holzbau und Baukonstruktion, R-Baumeister-Platz 1, Karlsruhe, 76131, Germany

ARTICLE INFO

Keywords:
Hardwood
Softwood
Experimental investigation
Rolling shear RS
Compression perpendicular to the grain CPG
Timber properties
EN 408 standard tests
Shear modulus
Elastic modulus

ABSTRACT

For an efficient material utilization of hardwood in engineering applications, mechanical properties and their relationships to the structure of the material are required. Herein, rolling shear (RS) and compression perpendicular to grain (CPG) stiffness and strength of southern Swedish beech, birch, and spruce were experimentally investigated. The experimental testing champaign consisted of (i) tests in three different ambient climates to quantify the moisture content (MC) influence and (ii) tests on two different characteristic scales to quantify the difference between the testing methods, and thus the influence of the annual ring structure. Since the analysis of variance for the investigated groups of different ambient climates yielded low statistical significance, a board-wise quantification method was applied. The effects of variations in density and annual ring structure were minimized by comparing samples from the same board. RS properties were equally influenced by moisture content in hardwood and spruce, while CPG properties of hardwood were stronger influenced by moisture content than spruce properties. Comparing results from the two different specimen sizes showed that the cylindrical orthotropic structure in the cross-section of boards substantially increased the effective RS strength as compared to smaller scale tests, whereas a weaker opposite trend was observed for CPG strength. RS and CPG stiffness were quite similar on both scales. The influence of the annual ring inclination on the material scale was further compared to multiscale material models for hardwood and softwood. The models showed that hardwood properties are stronger influenced by the density and much less by the annual ring inclination than properties of spruce, in agreement with the experimental analysis.

1. Introduction

European forests are undergoing significant changes, with a notable increase in the share of hardwood from deciduous trees. This trend is observed not only in Central Europe but also in Northern Europe, including Sweden. The shift towards hardwood, such as birch and beech, is driven by various ecological, economic, and social factors [1]. Especially in Sweden, not only climate adaptation but also increased biodiversity is a driving factor in the restoration and sustainable management of forests [2]. Increasing species admixture greatly reduces the risks of forest damages under unfavorable climate conditions [3]. Increasing temperatures and precipitation during the growth periods affect the growth rates of hardwood positively and the growth rate of softwood negatively [4]. Thus, the wood supply from the Scandinavian forests is changing [5]. In Sweden, hardwoods constitute about 20% of the forest composition. Birch accounts for approximately 13% of the standing volume, while other broadleaf trees, including beech, make up around 7% [6]. Softwood such as spruce and pine constitute about 80% of the forest composition [7]. Despite their superior mechanical properties compared to softwoods, most hardwoods are currently utilized for energy and paper production, rather than for high-valued engineered wood products for timber structures [8]. Sawn products constitute less than one percent of the yearly, industrially used hardwood in Sweden. Engineered wood products for construction are almost exclusively produced of softwoods, mainly of spruce and

* Corresponding author at: Department of Building Technology, Linnaeus University, Universitetsplatsen 1, Växjö, 35195, Sweden.
E-mail addresses: eva.binder@lnu.se (E. Binder), elisabet.kuck@kit.edu (E. Kuck), christian.bertram@kit.edu (C. Bertram), zijad.shehadeh@lnu.se (Z. Shehadeh), michael.schweigler@lnu.se (M. Schweigler), carmen.sandhaas@kit.edu (C. Sandhaas), thomas.bader@lnu.se (T.K. Bader).

https://doi.org/10.1016/j.conbuildmat.2026.147142
Received 17 December 2025; Received in revised form 16 June 2026; Accepted 17 June 2026
Available online 2 July 2026

pine. The potential for using hardwood in products, such as Glued-Laminated Timber (GLT) and Cross-Laminated Timber (CLT), remains largely unexploited.

For the use of hardwood in engineered wood products, a thorough understanding of the material behavior and influences of climate conditions and long-term effects are indispensable. For the effective use of hardwoods in engineered wood products, particularly CLT, understanding the rolling shear stiffness and strength, as well as the compression perpendicular to the grain stiffness and strength, is crucial [9–14]. Mainly due to their higher densities, hardwood species show higher stiffness and strength, clearly exceeding those of softwood. These properties could be exploited in the design of efficient truss structures or in the strengthening and reinforcement of engineered wood products with increased strength perpendicular to the grain, as well as the shear strength. The use of hardwood in center layers in hybrid CLT was shown to considerably improve the effective out-of-plane bending stiffness due to the higher rolling shear properties of hardwood [15]. Incorporating hardwood lamellas into glued laminated timber (GLT) beams significantly enhances their strength and stiffness compared to traditional softwood-only configurations [16]. However, hardwood species also have disadvantages that still hamper their use in the building sector, as for example increased shrinkage and swelling compared to softwood species [17,18] or different production chain requirements compared to softwood.

Al-musawi et al. [19] investigated the compressive strength in longitudinal, radial, and tangential direction of birch and beech at different moisture contents amongst other influence factors. Their experimental results at 20 °C confirmed the generally expected increase in strength with decreasing moisture content. Boruvka et al. [20] investigated the static and dynamic bending properties perpendicular to the grain of softwood and hardwood. They identified the elastic stiffness of birch and beech amongst other species. Milch et al. [21] and Niemz et al. [22] investigated stiffness and strength properties of European beech in longitudinal, radial and tangential directions at 65% relative humidity (RH) at 20 °C. Ehrhart and Brandner [13] investigated rolling shear properties of European soft- and hardwood with different test configurations, as these properties have gained importance in the use of cross laminated timber. Among other wood species, they investigated rolling shear strength and stiffness of birch and beech.

Wood has a hierarchically organized microstructure from the wood polymers cellulose, lignin and hemicelluloses to the cellular clear wood structure [23]. On a macroscopic scale of structural timber boards, the cylindrical annular ring structure of trees has a significant influence on the effective rolling shear and compression perpendicular to the grain behavior [24]. The influence of the annual ring orientation on the effective tensile and compressive stiffness of common ash clear wood in the transverse plane was shown in [25]. The influence of annual ring number and specimen size on the stiffness of poplar clear wood was shown in [26]. An increased size of wood specimens was shown to result in a decreased tension strength perpendicular to the grain due to a more inhomogeneous stress field caused by the cylindrically orthotropic material behavior [27]. At the clear wood scale, however, a rectangular orthotropic material behavior is commonly assumed [18,28]. There are different test configurations for the mechanical behavior of clear wood [18–22,29,30] and structural timber boards or products [11–14] but hardly any systematic analysis of the relationship between the determined properties. Such relationships can be described by means of (micro)mechanical models [31,32] but require thorough experimental datasets for model validation.

To expand the knowledge base on the material properties of hardwood and their relationships with the structure of the material, this paper aims to experimentally investigate the effective stiffness and strength of birch and beech from southern Sweden under compression perpendicular to the grain (CPG) and rolling shear (RS), including spruce as a reference material. In addition, the objective of this paper is to quantify the moisture content dependence of these effective material properties by testing samples under different climatic conditions. To assess the influence of test methods and specimen size, as well as the influence of the annual ring structure on effective material properties, smaller specimens at the material scale and larger specimens at the structural timber board scale are investigated. By addressing these objectives, this research contributes to the sustainable and efficient use of hardwoods in engineered wood products for timber structures.

2. Material

2.1. Investigated wood material

Beech (*Fagus sylvatica L.*), birch (*Betula pendula* and *Betula pubescens*), and spruce (*Picea abies*) boards were delivered from different sawmills in southern Sweden. The material represents a broad variation from different origins rather than a narrow selection from specific sites. Thus, boards were sawn from different radial and longitudinal positions across multiple logs, resulting in material comprising both sapwood and heartwood and exhibiting substantial variability in annual ring characteristics. The boards were first conditioned to the indoor lab hall climate at Linnaeus University before being sorted, labeled, and prepared for distribution between the two involved laboratories, namely the Research Center for Steel, Timber, and Masonry at Karlsruhe Institute of Technology in Germany and the Department of Building Technology at Linnaeus University in Sweden. The tests related to the board scale were performed in Germany and thus approximately two thirds of each board were sent for that purpose, while one third of each board stayed in Sweden to perform the experiments on the material scale, see Fig. 1. In order to generally characterize the investigated material, density and dynamic modulus of elasticity (MOE_{dyn}) were determined for every board destined for tests on the board scale. For the material-scale part of the same board, it was assumed that the density and MOE_{dyn} are not substantially deviating from the other part of the board.

The densities of the 37 boards (11 beech + 13 birch + 13 spruce) were determined by measuring weight and geometry of each board. The width varied between 186 and 363 mm, the thickness varied between 40 and 72 mm, and length varied between 1500 and 2020 mm. The mean wet densities were 711 kg/m^3 with a coefficient of variation (CV) of 5.11% of the beech boards, 644 kg/m^3 with a CV of 7.93% of the birch boards, and 463 kg/m^3 with a CV of 2.80% of the spruce boards. As expected from the broad origin of the material, the hardwood species showed a higher CV than the reference species spruce, and the range between maximum and minimum density of the boards was quite large and overlapping between the two hardwood species between 660 and 720 kg/m^3, see Table 1.

To identify the longitudinal vibration frequency f, the device GrindoSonic® MK7 was used. With the known density ρ and the length of the board l, the dynamic modulus of elasticity MOE_{dyn} was then determined as [33]

$$MOE_{dyn} = 4 \cdot f^2 \cdot l^2 \cdot \rho . \quad (1)$$

Mean dynamic moduli of elasticity (MOE_{dyn}) parallel to the grain of 13.3 GPa, 15.7 GPa, and 11.9 GPa were measured for beech, birch, and spruce, respectively, see Table 1. Considering the mean board densities of 711 kg/m^3, 644 kg/m^3, 463 kg/m^3 for beech, birch, and spruce, shows that the mean values of MOE_{dyn} are not only influenced by the mean board densities but also by the different microstructure of the wood species, and especially the amount of ray cells in the hardwood species [32,34].

Comparing MOE_{dyn} with literature showed that for beech, MOE_{dyn} is a bit lower than the 14.9 GPa for a density of 701 kg/m^3 identified by Ehrhart et al. [35], a bit higher than the 10.8 GPa for a density of 590 kg/m^3 identified by Guntekin et al. [36], and within the range of 12.8 GPa to 14.9 GPa for densities from 667 kg/m^3 to 681 kg/m^3

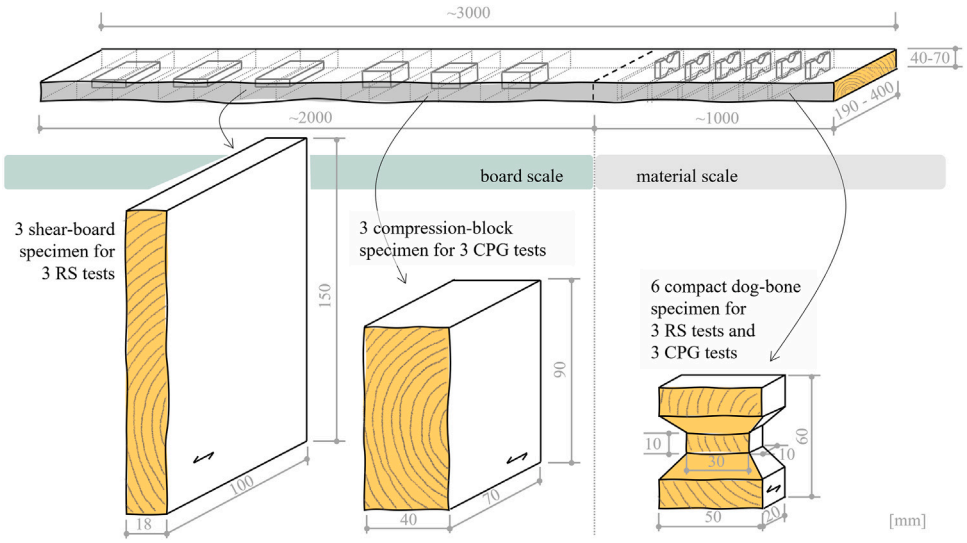

Fig. 1. Overview of specimen cut from one board with dimensions of the different types of specimens and targeted number of specimens.

Table 1
General characterization of the investigated boards by wet density and dynamic modulus of elasticity (MOE_{dyn}) in grain direction: mean values with coefficient of variation (CV), maximum and minimum values.

	beech	birch	spruce
density:			
mean value [kg/m³]	711	644	463
CV [%]	5.1	7.9	2.8
min. [kg/m³]	661	541	426
max. [kg/m³]	821	718	480
MOE_{dyn} in grain direction:			
mean value [MPa]	13 270	15 710	11 920
CV [%]	13.6	12.9	14.9
min. [MPa]	9 849	12 523	8 658
max. [MPa]	16 556	19 507	14 962

identified by Rais et al. [37]. For birch, MOE_{dyn} also seems low compared to Johansson et al. [38], who measured 16.2 GPa for 617 kg/m³, but still within a reasonable range looking at the data provided by Kollmann et al. [39] with a MOE_{dyn} of 10 GPa to 15 GPa at densities from 550 kg/m³ to 650 kg/m³. MOE_{dyn} of spruce is within the range of 10.9 GPa to 13.9 GPa for densities between 435 kg/m³ and 474 kg/m³, determined by Olsson et al. [9].

2.2. Test specimens and characteristic material scales

To follow standardized test protocols from EN 408 [40] for structural applications, a cross-section perpendicular to the grain of 150 mm by 18 mm was considered for rolling shear (RS) tests and a cross-section of 90 mm by 40 mm was chosen for compression perpendicular to the grain (CPG) tests, see Fig. 1. These are typical dimensions at the timber board scale, which however were used with a modification of the experimental setup according to EN 408 [40], as explained later.

In order to investigate the effect of the cylindrical orthotropy on the stiffness and strength of the boards, in addition, smaller specimens were tested on the material scale. For those specimens, it was assumed that the cylindrical orthotropy had a negligible influence, and the annual ring structure was approximated by a mean inclination of a rectangular orthotropic material behavior in the investigated part of the specimens. On this material scale, a cross-section of 30 mm by 10 mm (neck area of compact dog-bone specimens with overall dimensions of 50 mm by 60 mm) was investigated for RS as well as for CPG, see Fig. 1. In order to compare wood properties of the same board at two different characteristic scales and at three different ambient climates, 12 specimens were cut from each board, see Fig. 1. All specimens were prepared from defect-free clear wood. Before producing the final specimens, the material was cut into smaller pieces and stored in rooms or chambers with controlled climate to pre-condition the specimens at the intended ambient climate (more details see Section 2.3), until an equilibrium moisture content was reached, and to avoid cracks during the drying process. In total, 341 specimens were investigated in 36 different test groups (3 wood species × 2 loading conditions × 3 climates × 2 specimen sizes) in this study. The density was determined for each specimen and the mean densities of each group with CV are listed in Table 2. In the following, the preparation of the three different specimen types are described.

Shear-board specimens

The specimens for RS tests on the board scale were made of three timber layers, which were glued together crosswise by trained staff according to the recommendations of the adhesive manufacturer. After applying a primer a polyurethan adhesive was used for bonding and a visual inspection showed an adhesive layer thickness of less than 0.3 mm. The steel side members in the test setup for shear in grain direction according to EN 408 [40] were replaced by timber. Thus, specimens for an inclined compression test with an angle of 14° to the vertical axis were produced for RS testing of the middle layer. The thickness of the middle layer was 18 mm due to available board cross-sections. The height of the middle layer was 150 mm and the width of the specimens was 100 mm.

Preliminary tests on beech, using side layers made of timber and steel, were conducted with middle layers cut from the same board in order to ensure comparability. The results showed that the material of the side layers had no substantial influence on the rolling shear strength, but had an influence on the rolling shear stiffness, see Table 3. Similar conclusions were drawn by Mestek [41] and Nero et al. [42]. This is due to the higher stiffness of steel layers and a more even load transfer than with timber side layers. Based on the available materials and feasibility, the test setup with side layers in timber was selected, since it corresponds to a CLT setup. Due to their ease of fabrication, timber side layers are advantageous compared to steel layers and, as shown by findings of Collins and Fink [43], are suitable for rollings shear testing. By measuring the deformations in the central area of the board subjected to rolling shear, local effects in the load application area are minimized, but the determined stiffness can be considered a lower limit, as the actual timber board stiffness tends to be underestimated with this test setup.

Table 2
Tested specimens in the 36 groups (only those considered for board-wise evaluation): number of specimens (n), mean wet density [kg/m³] with CV in brackets, and mean MC [%] with CV [%] in brackets for each group (standard (std.) ambient climate).

		board scale						material scale					
amb. climate (RH)		dry (40%)		std. (65%)		wet (85%[a])		dry (40%)		std. (65%)		wet (85%)	
beech	**RS** number of spec.	9		9		8		11		10		10	
	density	713	(4.9)	718	(5.5)	715	(5.1)	684	(6.7)	687	(7.0)	710	(5.1)
	MC	8.7	(1.4)	11.8	(4.3)	15.0	(1.8)	8.7	(1.7)	12.4	(4.1)	16.9	(2.3)
	CPG number of spec.	10		10		10		10		8		9	
	density	703	(6.3)	705	(5.8)	710	(5.1)	670	(7.1)	684	(6.3)	703	(8.5)
	MC	8.6	(1.2)	12.2	(5.9)	15.1	(2.5)	8.3	(4.4)	12.4	(5.4)	17.0	(2.0)
birch	**RS** number of spec.	7		5		6		10		10		10	
	density	650	(4.3)	644	(10.3)	648	(8.9)	597	(8.9)	613	(9.7)	618	(11.3)
	MC	8.3	(0.8)	11.2	(1.6)	14.7	(0.7)	8.5	(1.5)	11.7	(1.7)	16.7	(1.3)
	CPG number of spec.	13		13		13		10		10		10	
	density	640	(8.3)	654	(9.2)	663	(9.2)	595	(10.1)	605	(11.2)	616	(10.0)
	MC	8.4	(1.4)	11.6	(1.8)	14.8	(0.8)	8.1	(2.4)	11.8	(2.1)	16.7	(1.6)
spruce	**RS** number of spec.	3		8		8		10		8		10	
	density	452	(5.1)	465	(1.9)	468	(3.5)	434	(9.3)	435	(6.5)	445	(6.5)
	MC	9.2	(1.7)	11.7	(1.5)	15.2	(0.5)	9.3	(1.6)	12.5	(0.8)	17.1	(0.9)
	CPG number of spec.	9		12		12		10		10		10	
	density	450	(3.2)	458	(3.2)	463	(2.8)	437	(6.3)	431	(7.6)	443	(8.3)
	MC	9.1	(1.0)	11.9	(1.8)	15.2	(1.0)	9.4	(1.5)	12.5	(1.0)	17.2	(0.9)

[a] The target relative humidity was not achieved during conditioning due to a malfunction.

Table 3
Pre-test results for RS tests on the board scale: comparison of beech shear-board specimens with timber and steel outer layers.

timber side layers:			
RS stiffness [MPa]	228	226	220
RS strength [MPa]	5.8	5.6	6.7
steel side layers:			
RS stiffness [MPa]	339	307	327
RS strength [MPa]	5.9	5.2	2.4[a]

[a] adhesive layer failed.

The test specimens were mostly single species, i.e. center layers of spruce glued to spruce side layers, and so on. Exceptions to this are the birch test specimens at the standard climate (65% RH). These were glued with side layers of beech laminated veneer lumber. These comparatively higher-strength side layers were used to prevent longitudinal shear failure of the side layers and to reduce indentations in the load application area.

Compression-block specimens

The height and width of the specimens for CPG testing on the board scale were 90 mm and 70 mm, respectively, following the EN 408 [40] standard. The thickness was slightly reduced to 40 mm instead of 45 mm prescribed in the standard, due to the smaller thickness of the boards.

Compact dog-bone specimens

Dog-bone specimens were used for testing RS and CPG on the material scale, as this shape creates an even strain distribution in the neck area of the specimens [29]. The dog-bones were milled out of conditioned slices of the different boards by a computer numerical controlled (CNC) machine. For investigating the properties on the material scale, the goal was to avoid the influence of the curvature of the annual rings and thus the position of the compact dog-bone specimen on the board slice was chosen so that the curvature of the annual rings in the neck area was as small as possible. The front and back surfaces of the dog-bones were sandpapered in preparation for the optical measurements, before mass and geometry of the specimens were measured. The speckle pattern was sprayed in two steps on one side of the specimen - first with a white ground coat and then producing black speckles. After applying the pattern, the mass was taken again to quantify the amount of applied paint. The wet density was determined with the mass of the conditioned specimen before testing without paint and the calculated volume.

Since the specimens were cut from boards with different origins in the tree, the specimens had different material orientations between the radial and tangential directions. The average annual ring inclination in the neck area of each compact dog-bone specimen was identified by loading a picture of the surface in a CAD software (AutoCAD Architecture 2023) and drawing an average line fitting the tangential direction of the annual rings and a reference line at the base of the specimen. The average annual ring inclination was estimated as the angle between those two lines, measured in the CAD software. The annual ring inclination varied between 0° (radial direction) and 90° (tangential direction) in all investigated groups.

2.3. Investigated ambient climates

The investigation focused on the mechanical properties at three different constant relative humidity levels. Mechanical properties were investigated at:

- Standard climate with 65% relative humidity (RH) at 20 °C, allowing to link the results to most documented experiments in literature; representing service class 1 according to Eurocode 5 [44]; resulting average MC of 12.2% for beech, 11.6% for birch, and 12.2% for spruce;
- Dry climate with 40% RH at 20 °C, representing a common ambient climate inside of buildings, especially during winter time; resulting average MC of 8.5% for beech, 8.3% for birch, and 9.3% for spruce;
- Wet climate with 85% RH at 20 °C, representing a common ambient climate for structures outside, but protected from direct rain, or rooms inside a building with high relative humidity, like bathrooms or kitchens; representing service class 2 according to Eurocode 5 [44]; resulting average MC of 17.0% for beech, 16.7% for birch, and 17.2% for spruce. Target relative humidity was not reached for board-scale specimens because of a climate chamber controller malfunction, which resulted in a less humid ambient climate for conditioning. The requirements for reaching equilibrium MC were fulfilled and the evaluation of the experimental results was performed based on the individual MCs of the specimens.

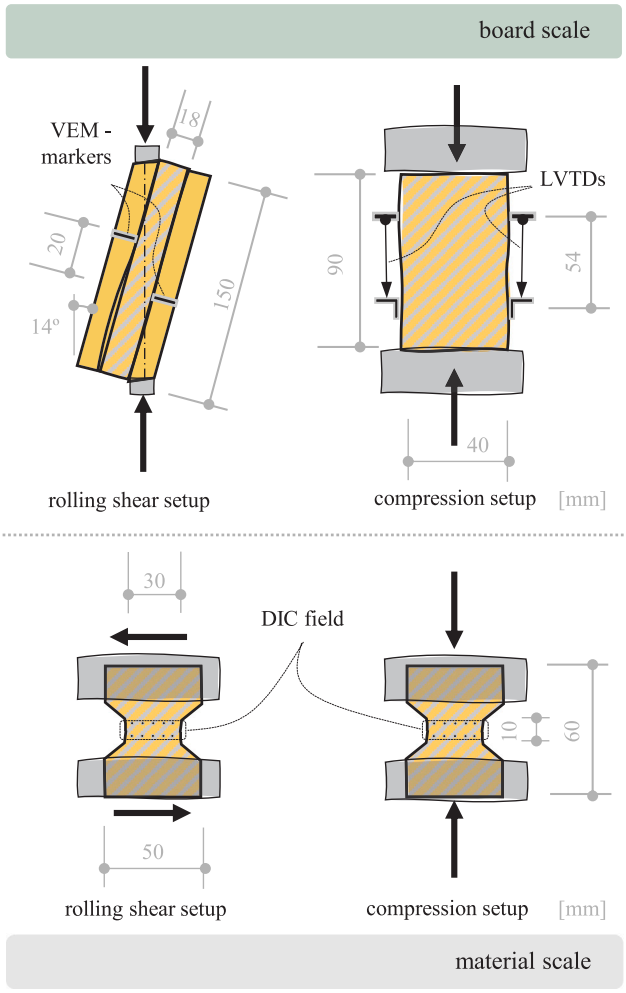

Fig. 2. Overview of experimental setups used on the board and material characteristic scales.

All specimens were cut at the respective laboratory and then stored in climate-controlled chambers to maintain the desired RH prior to testing. For the tests, the specimens were taken out of the climate chamber shortly before testing and tested promptly so that an increase or decrease in wood moisture content due to the laboratory conditions (service class 1) could be ruled out. Moisture conditioning was done in accordance with EN 408 [40] and the moisture content was determined by using the oven dry method according to EN 13183-1 standard [45]. MCs for each group are documented in Table 2. In the following, additional measurements of the specimen types are described.

Shear-board specimens

The moisture content was determined by cutting and drying samples from the middle layer after testing.

Compact dog-bone specimens

Between the steps of preparation, the specimens were always stored in the respective climate. In order to confirm the climate conditioning of the specimens between the preparation steps and before testing, the mass was measured every day until the mass difference was less than 0.2% on at least two following days, which was more strict than EN 408 requires. The MC was then calculated based on the oven-dry mass minus the weight of the paint and the mass of the conditioned specimen without paint.

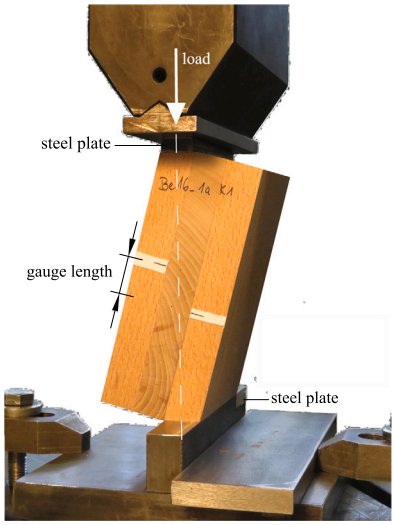

Fig. 3. RS testing on the board scale: experimental setup for RS.

3. Methods

In order to test the three different types of specimens on two characteristic scales, three different test setups were used, see Fig. 2. The evaluation of the experiments on both scales was done similarly, in order to make the results comparable. The following subsections describe the experimental setups and testing routines, as well as the applied evaluation procedures, including the calculation of strength and stiffness and their moisture content dependence.

3.1. Rolling shear testing at the board scale

Inclined compression tests were carried out to determine the strength and stiffness under rolling shear on the board scale. The test setup for the inclined compression tests (14° inclination) for the shear strength in grain direction according to EN 408 [40] was adapted and applied to rolling shear testing. As the load line runs through the center of gravity of the middle layer of the shear-board specimen, a uniaxial testing machine (Hegewald & Peschke inspekt 150) was used to apply the compression load. The load was applied at a constant loading rate with 0.6 mm/min without an unloading loop. Displacements parallel to the glue lines on both sides of the specimen were measured digitally via video extensometers (VEM). The VEM is a non-contact strain sensor connected to the testing software, specification RTSS (Real Time Strain Sensor) by the company Limess.

The measuring lines were placed 10 mm away from the center of gravity of the inner layer on opposite sides. Thus, the gauge length l equals 20 mm, see Fig. 3. The rolling shear strain, $\sigma_{RS.b}$, was determined based on the average displacements from VEMs on both sides of the specimen, Δl, and the gauge length as

$$\gamma_{RS.b} = \Delta l / l \,. \tag{2}$$

The measured force from the uniaxial testing machine F was divided by the cross-section area activated in rolling shear A_{RS}, i.e. 150 mm × 100 mm, to define the rolling shear stress on the board scale, $\sigma_{RS.b}$, as

$$\sigma_{RS.b} = \frac{F \cdot \cos(14°)}{A_{RS}} \,. \tag{3}$$

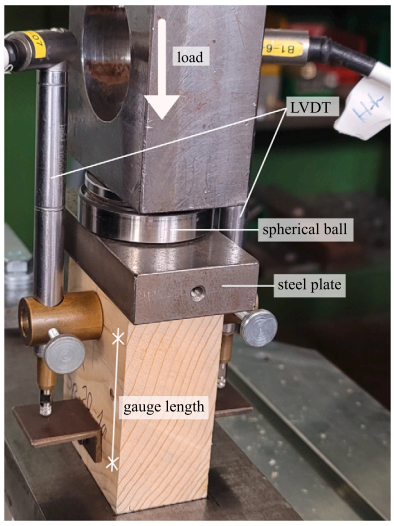

Fig. 4. CPG testing on the board scale: experimental setup in the uni-axial testing machine.

3.2. Compression perpendicular to the grain testing at the board scale

The determination of stiffness and strength in compression perpendicular to the grain on the board scale was conducted on the basis of EN 408 [40]. The load was applied by a uniaxial testing machine (Hegewald & Peschke inspekt 50) at a constant load rate, which was adjusted for each series (wood species and moisture content) so that the maximum load was reached in approximately 300 s. A spherical joint element (spherical ball) was positioned between the load application and a load-distributing steel plate at the top of the specimens, allowing the head of the specimens to freely rotate, see Fig. 4. Thus an even stress distribution was assumed and the compression perpendicular to the grain stress, $\sigma_{CPG.b}$, was calculated as

$$\sigma_{CPG.b} = F / A_{CPG}\,, \tag{4}$$

where F was the applied force during the test and A_{CPG} was the specimen's cross-section with 70 mm × 40 mm. In order to measure the vertical displacement of the specimens during testing, two LVDTs were placed in the center of two opposite faces to minimize any rotational effects. The initial gauge length of both LVDTs, h, was 54 mm. All data were recorded at a sampling rate of 5 Hz. The CPG strain, $\varepsilon_{CPG,b}$, was then determined as the mean relative displacement, Δh, divided by the gauge length as

$$\varepsilon_{CPG.b} = \Delta h / h\,. \tag{5}$$

3.3. Experimental test methods on the material scale

The experimental test setup used for CPG and for RS tests on the material scale is shown in Fig. 5. As there are no standards for these experiments, the applied experimental procedures, data acquisition, and evaluation are described in more detail in the following.

Experimental test procedure

A bi-axial test setup was applied for RS and CPG testing of the dog-bone shape specimens. The test setup in the bi-axial loading machine (MTS 322) was developed in Akter and Bader [29], where it was used for similar tests on Norway spruce with a digital image correlation system (DIC; Aramis from Gesellschaft für Optische Messtechnik mbH, Braunschweig, Germany) for measuring local deformations [46]. In this study, the dog-bone specimen were clamped between grip elements on the bottom and on the top side of the specimens, see Fig. 5. For

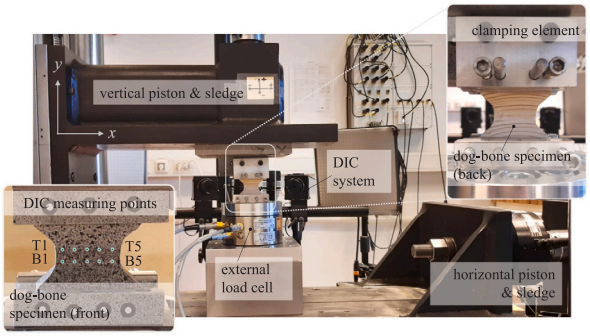

Fig. 5. RS and CPG testing on the material scale: experimental setup in the bi-axial testing machine, DIC measuring points.

Table 4
Estimated strength values for compression perpendicular to grain (CPG) and rolling shear (RS) based on existing data from literature [13,47].

	beech	birch	spruce
CPG strength [MPa]	12	7	6
RS strength [MPa]	6	3	2

mounting, the specimens were positioned between the lower clamps while the vertical sledge of the vertical piston was adjusted to a gap of approximately one millimeter between the sledge and the specimen. This allowed for a uniform gripping at the top and controlling and minimizing the gripping-induced forces. For the tests presented herein, the use of the DIC system was modified compared to originally developed setup in [29]. The field of view was 80 mm ×115 mm with a facet size of 19 px ×19 px and a grid spacing of 15 px, which resulted in a spacial resolution of approximately 36 px/mm. These settings allowed to choose specific points on the surface for the evaluation.

The loading procedure of the CPG tests consisted of four different load levels with an unloading in between — (i) two loading and unloading cycles up to 25% of the estimated strength (Table 4), reached within 10 s in force control mode, representing a stress-level typical for a quasi-permanent load level in a building structure, (ii) one loading and unloading cycle up to 50% of the estimated strength, reached within 15 s in force control mode, which should be within the elastic material behavior, (iii) one loading up 1 mm of machine displacement approached with a displacement rate of 2 mm/min and a following unloading to zero force with the same displacement rate, that was aimed to result in an loading and unloading in the plastic regime of the material behavior, and (iv) the final loading with a rate of 2 mm/min up to either reaching the capacity of the used load-cell of 4.8 kN or a machine displacement of 8 mm, see Fig. 6(a). For CPG, the described loads were applied through the vertical actuator while the horizontal actuator was kept in force-control mode at zero force (F_H = 0 kN). Due to the imperfect structure of wood, this resulted in a horizontal sliding of the specimens during loading.

The loading procedure for the RS tests included three different load levels with similar aims as described for the compression tests — (i) two loading and unloading cycles up to 25% of the estimated strength (Table 4), reached within 10 s in force control mode, (ii) one loading and unloading cycle up to 50% of the estimated strength, reached within 10 s in force control mode, and (iii) the final loading with a displacement rate of 1 mm/min up to failure of the specimens, indicated by a sharp load drop or by reaching the limits of machine displacement at 10 mm and capacity of the load cell at 4 kN, see Fig. 6(b). For RS, the described loads were applied through the horizontal actuator while the vertical actuator was kept in force-control mode at zero force (F_V = 0 kN) and thus global lateral tension of the specimen was avoided. Whereat, local minor tensile effects due eccentricity of load application cannot be eliminated.

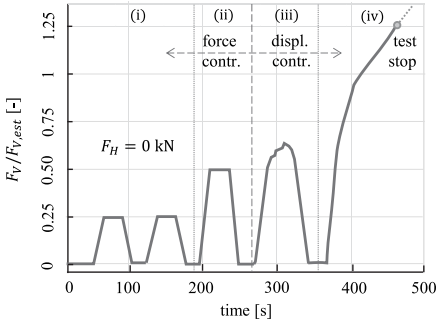

(a) Normalized vertical force over time for CPG testing.

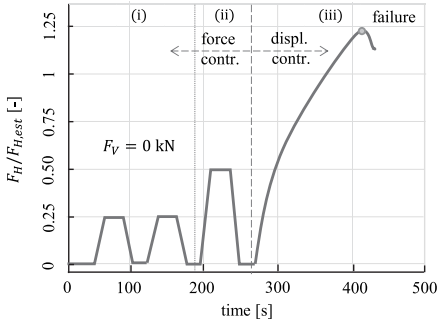

(b) Normalized horizontal force over time for RS testing.

Fig. 6. Schematic loading procedure for material-scale tests including the different loading sequences (i)–(iii) or (i)–(iv).

Data acquisition

For quantifying the local deformations during the loading sequence, ten measuring points arranged in two lines in the notched area of the dog-bone (T1 to T5 and B1 to B5) were defined, and their positions were extracted from the DIC measuring system as x-y-z coordinates, see Fig. 5. The DIC data acquisition was complemented by the horizontal and vertical force signals from the external multi-axial load cell (model GTM-69570, Gassmann Theiss Messtechnik, Germany) installed in the bi-axial loading machine. As the DIC was limited in the number of pictures of one continuous measuring sequence, a measuring rate of 2 Hz for the first two minutes of the test respectively the load cycles in the elastic testing regime, and a measuring rate of 1 Hz afterwards was used.

Stress and strain evaluation

Based on the experimental data, the measurement of the geometry of the notched section, and the assumption of a uniform stress distribution, the compressive stress, $\sigma_{CPG,m}$, and the shear stress, $\tau_{RS,m}$, were calculated by dividing the vertical force F_V and the horizontal force, F_H, by the cross-section area of the notched section of the specimens, A_n, as

$$\sigma_{CPG,m} = \frac{F_V}{A_n} \quad \text{and} \quad \tau_{RS,m} = \frac{F_H}{A_n} \quad . \tag{6}$$

The x-y-z coordinates of the 10 points from the experimental data were used to calculate a mean compressive and shear strain in the notched section of the dog-bone specimens. First, the mean distance between the upper five ($T1$ to $T5$) and the lower five measuring points ($B1$ to $B5$), see Fig. 5, h_0, was calculated based on y-coordinates before loading, y_0, as

$$h_0 = \frac{1}{5}\sum_{i=T1}^{T5} y_{0,i} - \frac{1}{5}\sum_{i=B1}^{B5} y_{0,i} \quad . \tag{7}$$

The relative displacements, in x- and y-directions between the upper and lower measuring points, are then identified as

$$\Delta x = \frac{1}{5}\sum_{i=T1}^{T5} [x_i - x_{0,i}] - \frac{1}{5}\sum_{i=B1}^{B5} [x_i - x_{0,i}] \quad \text{and} \tag{8}$$

$$\Delta y = \frac{1}{5}\sum_{i=T1}^{T5} [y_i - y_{0,i}] - \frac{1}{5}\sum_{i=B1}^{B5} [y_i - y_{0,i}] \quad . \tag{9}$$

Combining Eqs. (7) to (9) allows to calculate the mean normal strain in vertical direction, $\varepsilon_{CPG,m}$, and the mean shear strain, $\gamma_{RS,m}$, as

$$\varepsilon_{CPG,m} = \frac{\Delta y}{h_0} \quad \text{and} \quad \gamma_{RS,m} = \frac{\Delta x}{h_0} \quad . \tag{10}$$

3.4. Strength and stiffness evaluation

The determination of effective strength and stiffness in RS and CPG followed the EN 408 [40] for both characteristic scales.

As RS failure is a brittle failure mechanism, the maximum applied load can be identified by a sharp load drop in the force–displacement curve. The rolling shear strength, f_{RS}, is calculated based on the maximum applied load and the activated cross-section area of the individual specimen. The stiffness, G_{RS}, on the board scale was based on the average inclination of the load–displacement curves (considering the cross-section area and reference length afterwards) of the shear tests between load levels of 10 and 40% of the determined maximum force. The stiffness, G_{RS}, on the material scale was based on the secant modulus of the stress–strain curves of the shear tests between stress levels of 10 and 40% of the determined strength. In the context of rolling shear (RS), it should be emphasized that neither the material-scale nor the board-scale tests yield pure material stiffness and strength values due to unavoidable normal forces perpendicular to the global shear loading, which is also discussed in [13]. Systematic influences arising from the test configurations cannot be entirely excluded. For material-scale tests, the evaluation procedure for the deformations partially compensates for the effects of eccentric load application by calculating a mean displacement. However, local systematic influences can affect the initiation and progression of failure.

The CPG stiffness, E_{CPG}, was determined as the secant modulus of the load–displacement curves (considering the cross-section area and reference length afterwards) for the board scale and the stress–strain curves for the material scale of the compressive tests between load levels of 10 and 40% of the determined maximum load and strength respectively. The strength, f_{CPG}, itself was determined at the 1%-displacement and 1%-strain off-set respectively of the linear slope of the secant stiffness modulus, which required an iterative calculation.

3.5. Evaluation of moisture content dependence

The mechanical properties were investigated on different specimens with a wide variety of density, for a variety of different annual ring inclinations and curvatures and for three different climates. In addition to experiments, these three influence parameters (density, annual ring inclinations, and moisture content) were quantitatively investigated with validated multiscale models for spruce [31] and beech [32]. The comparison showed that the influences of density and the annual ring inclination variation are stronger than the influence of the investigated changes in moisture content, which does not allow for a straightforward evaluation of the experimental data. In order to minimize the influence of density variations and annual ring inclination, the evaluation of the influence of moisture content on mechanical properties was performed separately for each board.

Only boards with experimental results in at least two different climate classes were considered, as it was not possible to run all different

Table 5
Number of considered boards and resulting number of specimen (number in brackets) for the evaluation of moisture content dependence.

		beech	birch	spruce
RS	board scale	9 (26)	7 (18)	8 (19)
	material scale	11 (31)	10 (30)	10 (28)
CPG	board scale	10 (30)	13 (39)	12 (33)
	material scale	10 (27)	10 (30)	10 (30)

mechanical tests in all three ambient climates for all 37 boards. The number of boards and specimens considered in the evaluation of the moisture content dependence are documented in Table 5. The moisture content dependence for the four investigated mechanical properties (stiffness and strength in CPG and RS) on the two investigated characteristic scales (board scale and material scale) for each investigated species (beech, birch, and spruce) were evaluated, which resulted in moisture content dependencies in 12 categories of the material and board scale. These were quantified by a linear regression fitting the experimental results at the different moisture contents. The function 'polyfit', for a first order polynomial ($y = kx + d$), in the software Matlab [48] was used and the result for each board in each category was the inclination of the linear fit (k-value) and a shift of the linear fit at the theoretical moisture content of zero (d-value).

Based on the linear regression results for the individual boards, an average linear fit for each category was determined, as mean value of k- and d-values. To link these average fits with values from literature, the fit was evaluated at 12% moisture content (referred to as reference value, RV= $k_{\mathbf{mean}}12\% + d_{\mathbf{mean}}$) and the inclination was expressed as change of the investigated mechanical property per one percent change of moisture content.

3.6. Micromechanical modeling for assessment of experiments

Multiscale material models for wood allow to separate the influence of annual ring orientation, density, and moisture content on mechanical properties. A validated multiscale micromechanical model (MM-model) for the stiffness of softwood was presented by Bader et al. [31] and further extended to hardwood by de Borst and Bader [32]. The stiffness models were applied for the three investigated species to obtain the nine independent components of the stiffness tensor linked to longitudinal grain direction (L), radial direction (R), and tangential direction (T) of clear wood. The input parameters for the models were either dry or wet density and moisture content of the wood. In order to compare the models with the experimental results, the mean densities and MCs from RS and CPG from the material-scale specimens in the standard climate, see 'Mean values of tested specimens' in Table 6 were considered as input. The dry density, ρ_{dry}, was calculated according to [49] as

$$\rho_{dry} = \rho_{wet}\left(1 + \frac{u}{100} - 0.84\frac{u}{100}\frac{\rho_{wet}}{1\,\mathrm{g/cm^3}}\right)^{-1}, \tag{11}$$

where ρ_{wet} and u were the wet density and the MC (expressed as a number between zero and one). As the conditioning of the specimens resulted in different MCs, the main comparison with the model was done at a MC of 12%. Therefore, Eq. (11) was rearranged to calculate the reference wet density at 12% MC, which is the input parameter for the multiscale model for hardwood. These sets of input values are referred to as 'reference material' in Table 6.

To predict also the influence of the different experimentally investigated MCs and densities, MCs of 8% (representing the dry climate of conditioning) and 17% (representing the wet climate of conditioning) and upper and lower densities were evaluated in addition to the reference configuration. The upper and lower densities were defined based on the variation of density of the tested specimen of each species, see Table 6, by increasing and decreasing the reference density by a factor twice the CV respectively. The input values for the micromechanical models are listed in Table 6.

The influence of the inclination of the annual ring structure in the RT-plane, from 0° (R-direction) to 90°(T-direction), was predicted by rotating the RT-stiffness tensor components derived by the micromechanical model. The effective RS and CPG stiffnesses are plotted in Fig. 7 for beech and spruce only, as the MM-models were not validated for birch. The micromechanical calculations for birch were only used for a qualitative comparison with the experiments.

For comparing the MM-model predictions with the experimental results, an adaption to 12% MC and a normalization were done. The influence of the different MCs of the individual tests was compensated by calculating the value at 12% MC based on the determined linear moisture content dependence (k-values) according to Section 3.5, labeled as G^*_{RS}, f^*_{RS}, E^*_{CPG}, and f^*_{CPG} in the following. The normalization of the experimental values was done by RV at 12% from the material scale defined according to Section 3.5 and the MM-model was scaled with the stiffness at the mean annual ring inclination of the material-scale experiments.

3.7. Statistics for assessment of experiments

The statistically significant difference between the three climates in each test series was determined with a one-way analysis of variance (ANOVA). Based on the ANOVA of each test series, the statistical probability (P-value) the difference between the investigated climate classes occurred by chance was calculated with the function 'anova1' in the software Matlab [48]. The common limit of a P-value less than 0.05 to assume significance of the experimental results regarding the investigated climates was considered in the study.

4. Results and discussion

4.1. RS stiffness and strength

The mean values of the effective RS stiffness and strength were calculated for the investigated 18 groups (3 wood species, 2 characteristic scales, 3 ambient climates) and are documented in Table 7. The highest values are identified for the groups conditioned to the dry climate and the lowest values for groups conditioned to the wet climate, except for the strength at the material scale. Further evaluation of the moisture content dependence was done in Section 4.2. Comparing RS stiffness and strength of the investigated species, a general correlation between a higher stiffness and strength for increased density was confirmed, see Tables 2 and 7.

The correlation plots of the effective RS properties at the different investigated scales are presented in Fig. 8. For beech, the RS stiffness on the board scale is similar to the stiffness determined on material scale. RS stiffness of birch and spruce are 30% and 59% higher on the board scale than on the material scale. The board-scale tests led to higher RS strength values than the material-scale tests for both hardwood species, but not for spruce. Thus, the influence of the annual ring structure present at the board scale, increased the effective strength compared to the material scale by 80% on average for both hardwood species and only by 9% for spruce.

In literature documented earlier findings of RS stiffness and strength of the three investigated species are listed in Table 8. Interestingly, even if similar test setups were used, the RS stiffness of beech in literature is more than 50% higher than the results on the board scale presented herein, amounting to 232 MPa with a CV of 29% at a mean density of 718 kg/m^3 from Tables 2 and 7. As the used board-scale experimental setup with timber side layers tends to underestimate the RS stiffness of the tested timber board [41,42], this could be a cause for the differences with literature. Stiffness values of birch from literature are in good agreement with the experiments presented in this study, where the stiffness amounted to 192 MPa with a CV of 29% at a mean density of

Table 6
Mean values from the tested specimens and resulting input parameters for the MM-models for the 5 evaluated configurations.

	beech	birch	spruce
Mean values of tested specimens: acc. Tab. 2			
MC [%]	12.4	11.7	12.5
density at MC [kg/m^3]	686	609	437
mean CV of density [%]	6.7	10.5	7.4
Configuration 1: reference material			
MC [%]	12	12	12
density dry [kg/m^3]	651	580	405
density at MC [kg/m^3]	684	614	436
Configuration 2: dry material			
MC [%]	8	8	8
density dry [kg/m^3]	651	580	405
density at MC [kg/m^3]	674	603	426
Configuration 3: wet material			
MC [%]	17	17	17
density dry [kg/m^3]	651	580	405
density at MC [kg/m^3]	697	627	448
Configuration 4: upper density			
MC [%]	12	12	12
density dry [kg/m^3]	738	701	464
density at MC [kg/m^3]	775	742	500
Configuration 5: lower density			
MC [%]	12	12	12
density dry [kg/m^3]	565	459	345
density at MC [kg/m^3]	594	486	371

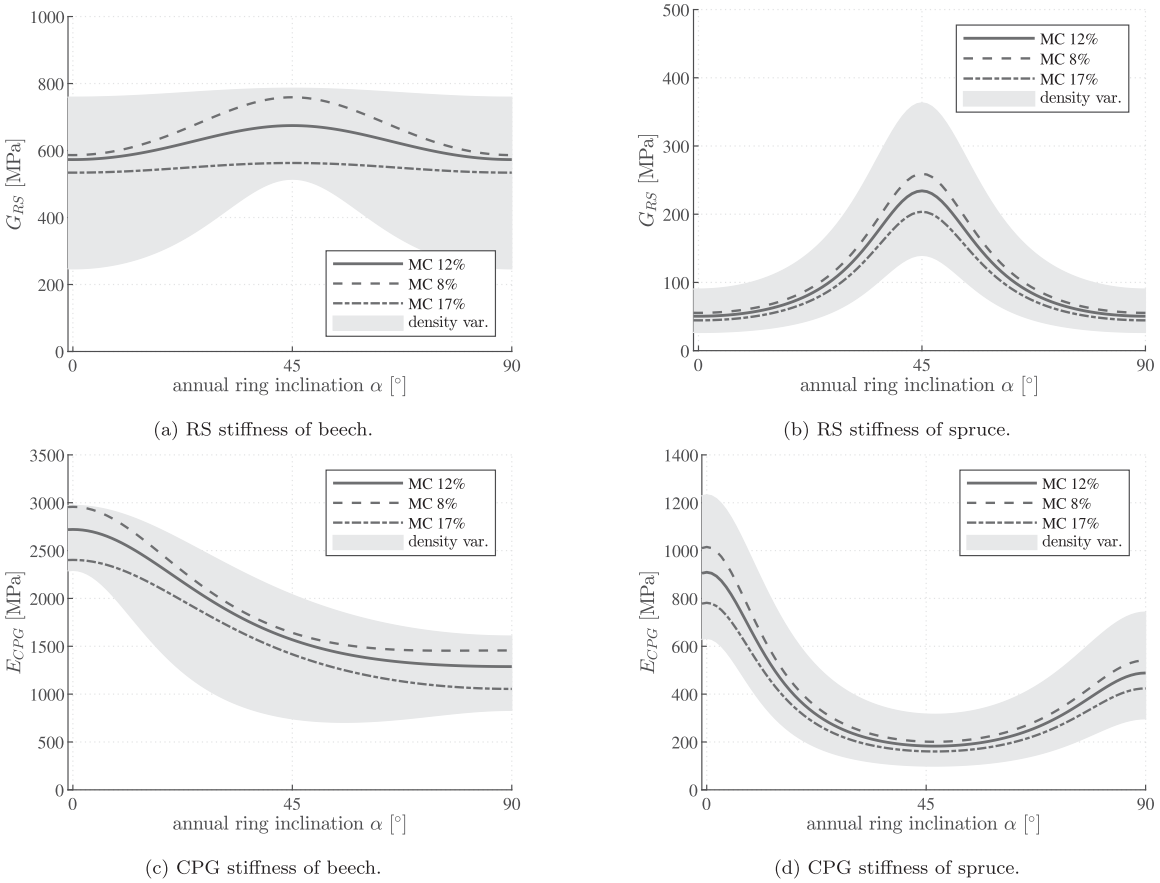

(a) RS stiffness of beech.

(b) RS stiffness of spruce.

(c) CPG stiffness of beech.

(d) CPG stiffness of spruce.

Fig. 7. Model prediction of the influence of the annual ring orientation on stiffness based on the validated MM-models in [31,32], considering different MC and density configurations listed in Table 6.

644 kg/m^3 as shown in Tables 2 and 7 from the standard climate. The RS stiffness of spruce in the literature were determined with different test setups and can be compared to the board-scale test results (98 MPa with CV 42% at 466 kg/m^3) and the material-scale results (55 MPa with CV 33% at 442 kg/m^3) presented herein. The experimental results confirmed the ranges found in literature, except from the results of Nero et al. [42], which were a bit lower.

As for RS strength of beech, the material tested herein was found to have a lower stiffness but a higher strength (7.0 MPa board scale with CV 18% at 718 kg/m^3) as compared to previous studies. For birch, the

Table 7
Experimental results on board and material scale for rolling shear (RS) for the three investigated climate conditions (dry- 40% RH, standard (std.)- 65% RH, wet- 85% RH): mean values [MPa] and coefficient of variation [%] in brackets for stiffness and strength.

RS		board scale						material scale					
ambient climate (RH)		dry (40%)		std. (65%)		wet (85%[a])		dry (40%)		std. (65%)		wet (85%)	
beech	number of tests	9		9		8		11		10		10	
	stiffness	259.5	(8.8)	231.7	(28.9)	216.8	(22.6)	259.3	(13.6)	235.0	(13.3)	201.6	(15.7)
	strength	7.7	(6.7)	7.0	(7.6)	6.0	(6.8)	4.0	(19.4)	4.5	(17.9)	4.4	(21.6)
birch	number of tests	7		5		6		10		10		10	
	stiffness	159.4	(13.7)	192.0	(28.7)	149.1	(18.3)	140.8	(28.3)	137.9	(28.3)	103.8	(31.8)
	strength	6.0	(8.6)	5.2	(13.9)	4.5	(10.0)	2.6	(18.0)	3.4	(15.7)	3.1	(20.3)
spruce	number of tests	3		8		8		10		8		10	
	stiffness	124.5	(23.8)	98.4	(41.5)	101.6	(28.7)	83.3	(29.2)	55.1	(33.3)	62.1	(46.2)
	strength	2.8	(28.5)	2.9	(26.6)	2.4	(2.8)	2.2	(29.5)	2.3	(19.3)	2.1	(21.0)

[a] The target relative humidity was not achieved during conditioning due to a malfunction.

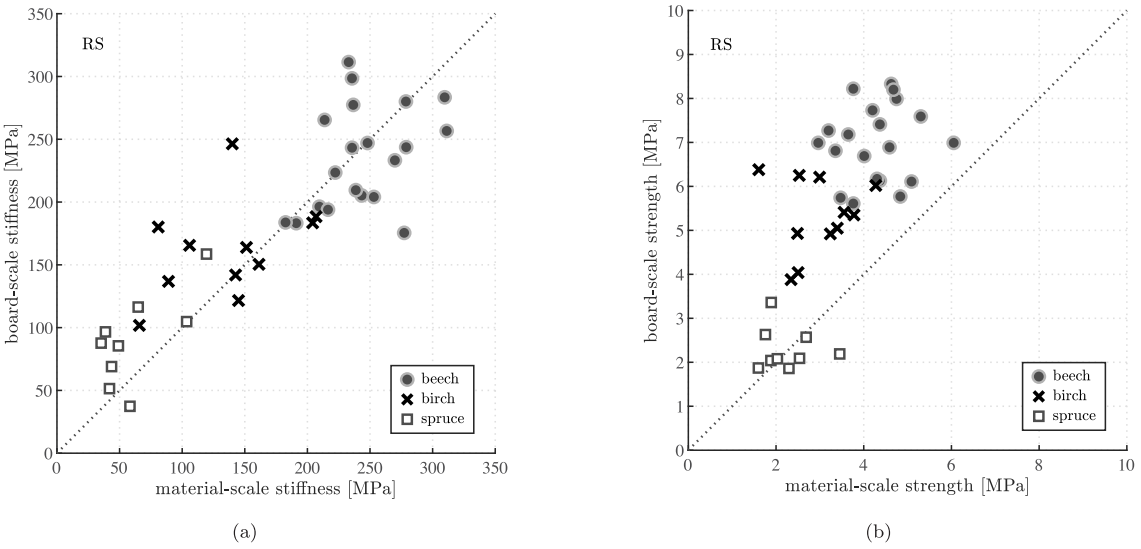

Fig. 8. Correlation plots of RS (a) stiffness and (b) strength at different scales: individual test results (markers) for beech, birch, and spruce.

Table 8
RS experiments in literature performed at standard climate: species, mean density, property (mean stiffness or strength values), corresponding coefficient of variation (CV), and the scale for comparison (board scale (b) or material scale (m)).

RS Literature reference	species	density [kg/m^3]	property	[MPa]	CV [%]	scale
Aicher et al. [50]	beech	669	stiffness	370	20	b
Niemz et al. [22]	beech	665	stiffness	380	–	b
Ehrhart & Brandner [13]	beech	720	stiffness	357	12	b
Ehrhart & Brandner [13]	birch	612	stiffness	188	19	b
Neuhaus [51]	spruce	460	stiffness	48	–	–
Görlacher [52]	spruce	450	stiffness	28–108	–	–
Hassel et al. [53]	spruce	452	stiffness	61–68	–	m
Flaig [54]	spruce	421	stiffness	99	74	–
Akter et al. [46]	spruce	465	stiffness	51	–	m
Perstorper [30]	spruce	–	stiffness	50–300	–	m
Ehrhart & Brandner [13]	spruce	439	stiffness	100	27	b
Nero et al. [42]	spruce	392	stiffness	33–44	3	b
Aicher et al. [50]	beech	669	strength	5.60	16	b
Ehrhart & Brandner [13]	beech	720	strength	5.37	9	b
Ehrhart & Brandner [13]	birch	612	strength	3.45	10	b
Mestek [41]	spruce	466	strength	2.13	24	–
Flaig [54]	spruce	421	strength	1.59	22	–
Ehrhart & Brandner [13]	spruce	439	strength	1.88	13	b
Nero et al. [42]	spruce	392	strength	0.79	5	b
Akter et al. [46]	spruce	465	strength	1.59	–	m

experimental data presented herein, with 5.2 MPa with a CV of 14% at a mean density of 644 kg/m^3 at the standard climate, is more than 50% higher than the results in [13]. The RS strength values for spruce were derived with different test setups in literature and the determined strengths on the board scale (2.9 MPa with CV 27% at 466 kg/m^3) and the material scale (2.3 MPa with CV 19% at 442 kg/m^3) are slightly higher than the literature data. For the board-scale experimental setup, the lamination aspect ratio of the tested shear board influences the RS strength [55]. Hence, this could explain higher strength values of this work compared to the experiential results from literature, as the shear-board thickness was 18 mm and thus smaller than EN 408 [40] requires.

The failure modes on board scale, showed cracks likewise either in radial or tangential direction. Even combined failure modes appeared. The crack path depended on the orientation of the annual rings of the individual specimen. It seems the shortest crack length to split the specimen either in radial or in tangential direction was the governing one, see Figs. 9 (a) and (b). As for the failure modes on the material scale, the cracks induced by the brittle RS failure were oriented in radial, tangential or combined direction, see Figs. 9 (c) and (d). Crack initiation was situated at the outer edge of the neck area, where despite the optimized shape of the specimen stress peaks might have occurred. In case of inclined annual rings, in most specimens, the crack propagated from the outer edge towards the clamping, see Fig. 9 (c). For vertical and horizontal annual ring patterns, a horizontal crack appeared, see Fig. 9 (d).

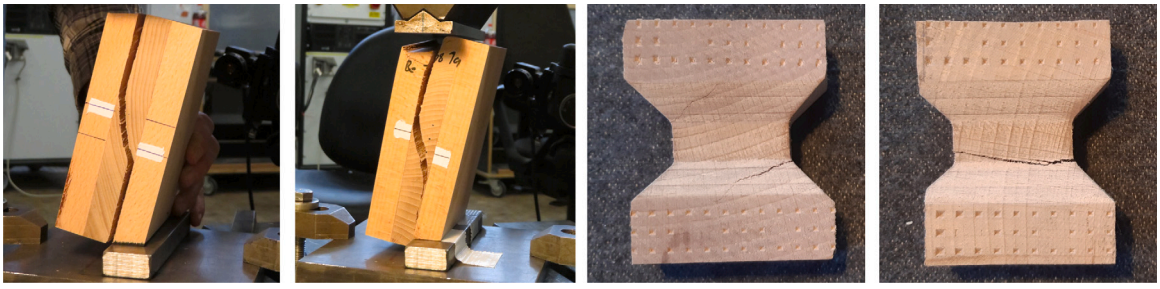

(a) (b) (c) (d)

Fig. 9. RS specimen with typical crack patterns: (a) board-scale specimen with tangential crack; (b) board-scale specimen with radial crack; (c) material-scale specimen with radial crack through the neck area; (d) material-scale specimen with tangential crack initiated in the corner of the neck area.

Table 9
P-values from one-way ANOVA testing the effect of group of 3 ambient climates for conditioning on the response variable (RS stiffness or RS strength).

RS	board scale			material scale		
p-values [-]	beech	birch	spruce	beech	birch	spruce
stiffness	0.1874	0.0769	0.5693	0.0016	0.0644	0.0266
strength	0.000003	0.000028	0.3100	0.2697	0.0116	0.4968

4.2. Influence of the moisture content on RS stiffness and strength

The variability between the dry, standard, and wet conditioned groups of specimens in comparison with the variability within in the group is tested with an ANOVA. The p-values larger than 0.05 of the ANOVA show that for more than half of the investigated categories, i.e. species, scale, stiffness, and strength, no significant influence of the moisture content is given, see Table 9. Considering the results from the multiscale modeling in Fig. 7, the missing significant difference can be ascribed to the more pronounced influence of density and annual ring orientation on stiffness of wood than differences in MCs. In order to quantify the dependence of the RS stiffness and strength on the moisture content, the board-wise evaluation method described in Section 3.5 was applied.

The average dependencies, which are expressed as k-value and RV at 12% MC, for the different categories are summarized in Table 10. Both RS stiffness and strength are shown as a function of the MC in Fig. 10. The influence of the MC is illustrated for each original timber board, from which several specimens were cut for testing at the two different characteristic scales and the different MCs. In addition, a regression over all data points is shown for the material-scale and the board-scale tests.

The MC dependence of the RS stiffness was more uniform for beech at board scale and material scale than for birch. For spruce the trend for the MC dependence was in opposite directions on the investigated scales. The CV values of the MC dependencies (k-values) were comparably high, see Table 10.

On the board scale of all species, the RS strength followed the same trend, but on the material scale the hardwood species showed an increasing strength with increasing MC in contrast to spruce with a decreasing strength with increasing MC, see Figs. 10 (b) and (d). Regarding this unexpected results of the hardwood specimens, it is worth looking at the results of the individual boards, where most of the boards show the expected trend, but only with a small dependence of strength on the MC. Worth mentioning as well, the very high CVs in Table 10 are linked to very low k-values.

It should be noted that the tests on both scales were performed in an unconditioned test climate after conditioning the specimens in climate rooms and climate chambers to the desired ambient climate. Thus, due to the open end grain of the specimens, and especially for the small size of the neck area of dog-bone specimens, it is possible that the testing climate influenced the MC of the specimens during testing.

Table 10
Linear moisture dependence of rolling shear (RS): absolute change of stiffness and strength per one percent increase of moisture content (k-value) with coefficient of variation (CV) and reference value (RV) at 12% moisture content and relative change compared to the RV [%/%$_{MC}$].

	board scale			material scale		
RS	beech	birch	spruce	beech	birch	spruce
stiffness k-value [MPa/%$_{MC}$]	−6.0	−2.6	1.6	−7.3	−4.7	−2.5
CV of k-value [%]	172	160	601	33	51	209
RV [MPa]	237.1	160.8	97.4	237.9	128.9	71.7
rel. change [%/%$_{MC}$]	2.5	1.6	−1.6	3.1	3.6	3.5
strength k-value [MPa/%$_{MC}$]	−0.23	−0.24	−0.10	0.049	0.045	−0.021
CV of k-value [%]	66	26	170	137	155	453
RV [MPa]	6.96	5.10	2.76	4.29	3.02	2.22
rel. change [%/%$_{MC}$]	3.3	4.7	3.6	−1.1	−1.5	0.9

Comparison of the MC dependence of RS properties of the three investigated species did not allow to distinguish between the hard- and softwood species when comparing the relative changes independent of the scale, see Table 10. If only the negative k-values are considered, the RS stiffness and strength decreases on average by 3%/%$_{MC}$. The comparison of the scales allows the assumption that the RS strength is stronger influenced by a MC change on the board scale than on the material scale whereat a MC change yields the opposite trend for the RS stiffness.

The MC dependence of the RS properties of spruce is hardly documented in the literature and, to the best of our knowledge, was not investigated at all for any hardwood species. In Akter et al. [46], RS stiffness and strength of spruce were investigated at 5 different ambient climates and third-order polynomial functions for the influence of MC on the RS stiffness and strength were developed. The shape of the polynomial functions for stiffness and strength are almost linear between 8 and 20% MC, and thus, the first derivatives at 12% MC are considered for comparison with this work, see Figs. 10(e) and (f). These values are close to the MC dependence of spruce measured herein (Table 10).

4.3. Influence of the annual ring inclination on RS stiffness and strength

As the analysis of the MC dependence indicated a strong influence of the testing method and yielded in general very high CV values (see

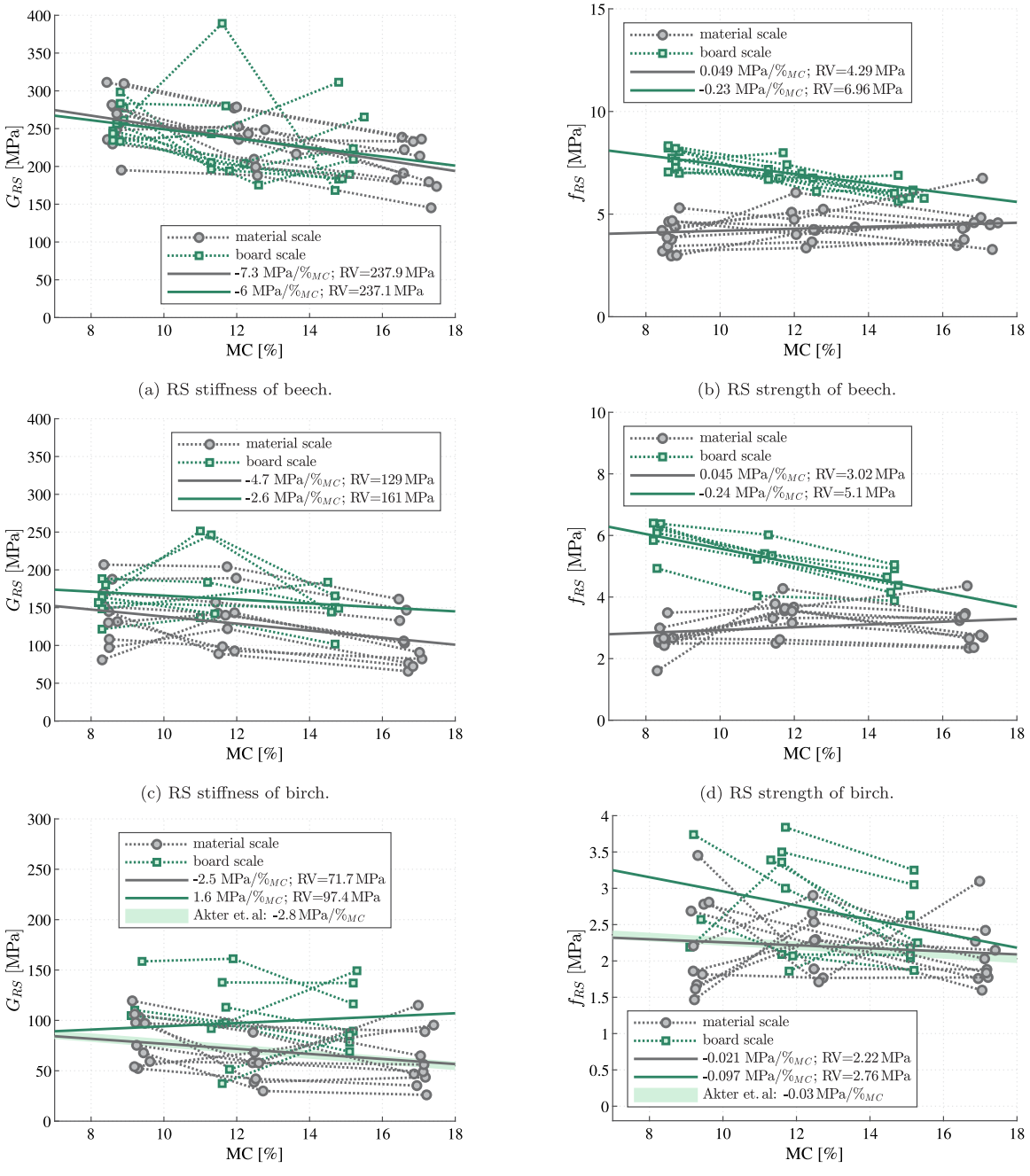

(a) RS stiffness of beech.

(b) RS strength of beech.

(c) RS stiffness of birch.

(d) RS strength of birch.

(e) RS stiffness of spruce.

(f) RS strength of spruce.

Fig. 10. Experimental results of RS stiffness G_{RS} and strength f_{RS}: individual test results (markers), board results (dotted lines between markers), and average group fit for board and material scale (continuous lines); available literature values for comparison (shaded area).

Table 10), an analysis regarding the influence of the annual ring structure was conducted in addition while minimizing the dependence of the MC. Fig. 11 shows the normalized (effective) RS stiffness and strength as a function of the annual ring inclination of the dog-bone specimens (material scale) and the relative properties at the board scale, as well as the trend lines for RS stiffness predicted by the MM-model.

For beech and birch, the RS stiffness was not distinctly influenced by the annual ring inclination. The results vary in a range of ±20% for beech and ±50% for birch (Figs. 11(a) and (c)), but a clear trend with respect to the annual ring inclination was not obvious from the experiments. A different result was found for spruce, where a clear peak was visible around an annual ring inclination of 45° and the lowest RS stiffness was found around 0° and 90° (Fig. 11(e)).

Aicher and Dill-Langer [24] did a theoretical investigation on the influence of the sawing patterns on the RS stiffness of a board (test specimen) based on finite element modeling. Their results are in good agreement with the MM-model predicted trends of the RS stiffness of spruce (Fig. 7(b)) and the corresponding material-scale results presented in Fig. 11(e). The theoretical results of 3 boards with different pith locations in [24] were between the boundaries found for different annual ring inclinations, which agrees well with the comparison of board-scale and material-scale test results herein.

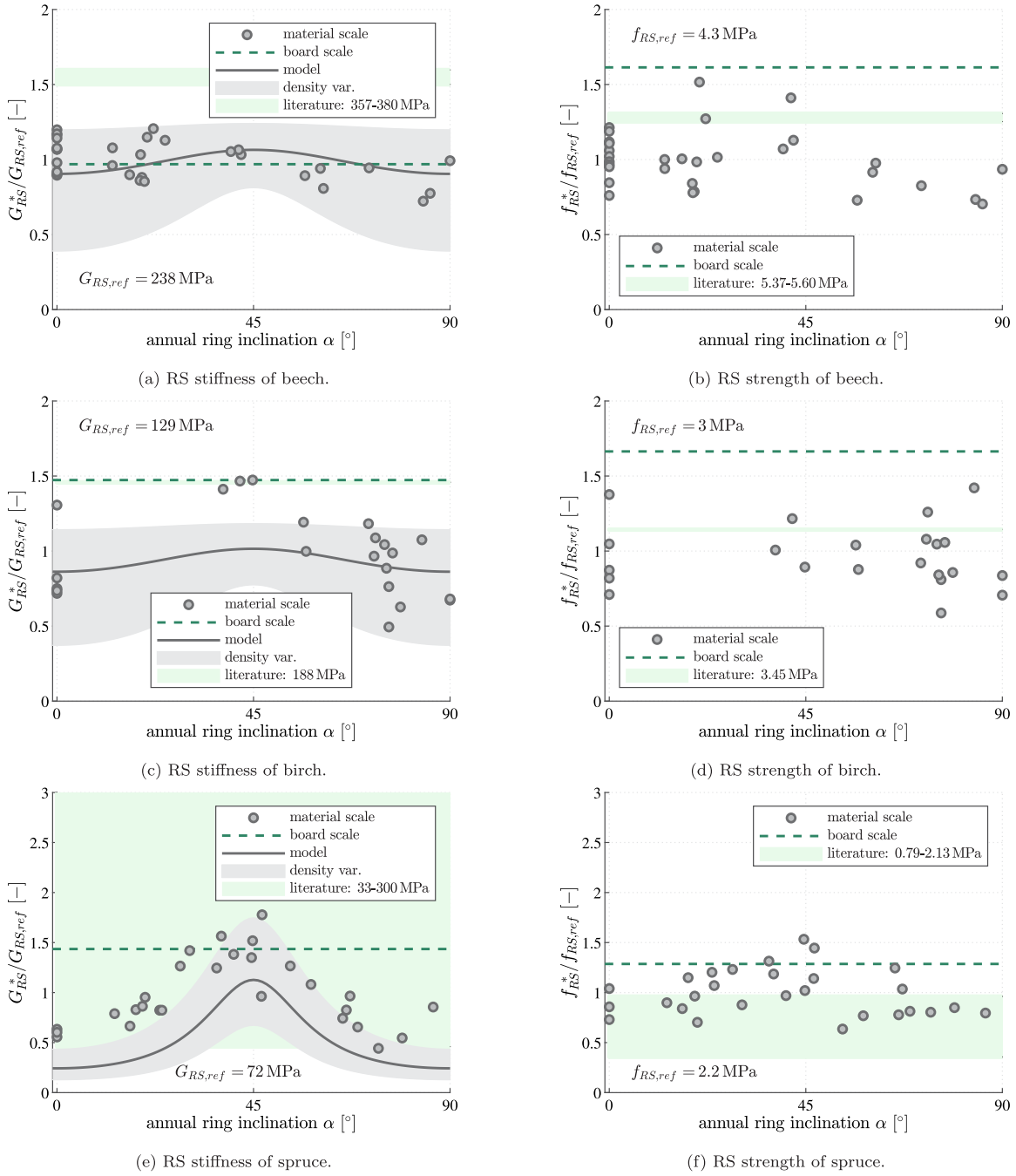

Fig. 11. Influence of annual ring inclination on normalized RS stiffness $G^*_{RS}/G_{RS,ref}$ and normalized RS strength $f^*_{RS}/f_{RS,ref}$: individual test results on the material scale (markers), results on the board scale from Table 7 (dashed green line — mean value standard climate), model prediction (continuous line — mean value standard climate; light gray shaded area — density variation between upper and lower density), and strength and stiffness range from literature listed in Table 8 (light green shaded area).

For beech, as a hardwood species with a higher density than spruce, Aicher et al. [50] showed that there is a significantly smaller influence of the annual ring inclination on the RS stiffness. This is a result of the lower stiffness ratio between radial stiffness and RS stiffness, and a more isotropic behavior in the transverse plane of beech than of spruce. The stiffness ratio is around 20 to 40 for spruce but only 3 to 5 for beech. The smaller influence of the annual ring orientation on the RS stiffness of beech was confirmed with experimental investigations. These results are in agreement with the MM-modeling results (Fig. 7(a)) and the experimentally undetectable influence of the annual ring inclination on the RS stiffness on the material scale, see Figs. 11(a) and (c). Experimental detection of this effect would likely require a more controlled sampling strategy with reduced variability in the raw material.

The density was earlier shown to have an influence on the RS stiffness and strength of hardwood but not of spruce [13]. This supports the findings herein, which for beech and birch indicated a stronger influence of the density on the RS stiffness and strength than of the annual ring inclination.

With a new dynamic testing method, Perstorper [30] investigated the influence of the annual ring inclination in small spruce specimens (10 × 14 × 60 mm) on the RS stiffness. The lowest values were found

Table 11
Experimental results on board and material scale for compression perpendicular to the grain (CPG) for the three investigated climate conditions (dry- 40% RH, standard (std.)- 65% RH, wet- 85% RH): mean values [MPa] and coefficient of variation [%] in brackets for stiffness and strength.

CPG		board scale						material scale					
ambient climate (RH)		dry (40%)		std. (65%)		wet (85%[a])		dry (40%)		std. (65%)		wet (85%)	
beech	number of tests	10		10		10		10		8		9	
	stiffness	1739	(22.7)	1623	(24.2)	1413	(24.0)	1737	(33.1)	1382	(24.8)	1290	(38.3)
	strength	12.0	(15.9)	9.9	(15.4)	8.7	(16.7)	15.2	(27.8)	11.3	(21.3)	10.5	(32.6)
birch	number of tests	13		13		13		10		10		10	
	stiffness	853	(24.6)	807	(26.6)	653	(27.2)	771	(12.1)	629	(11.9)	524	(16.5)
	strength	7.5	(22.2)	6.6	(23.1)	5.4	(20.9)	8.1	(16.8)	6.9	(10.6)	5.7	(13.5)
spruce	number of tests	9		12		12		10		10		10	
	stiffness	382	(73.9)	350	(64.5)	303	(61.3)	377	(30.2)	297	(43.4)	324	(51.4)
	strength	3.4	(19.7)	3.0	(18.8)	2.8	(20.6)	4.1	(17.3)	4.0	(16.8)	3.6	(21.2)

[a] The target relative humidity was not achieved during conditioning due to a malfunction.

close to 0° and 90° and the highest values at 45° annual ring inclination, which agrees well with the experimental results on the material scale in Fig. 11(e).

4.4. Further aspects of the RS stiffness and strength investigation

The conducted experiments aimed to extend the experimental data on RS properties by testing hardwood and softwood from different origins in southern Sweden. This resulted in a large variety of board densities and annual ring orientations and curvatures, and distributions of heart- and sapwood over the cross-section of the board, which ultimately led to a large variation of the experimental results in each of the 18 investigated categories, see Table 10. Furthermore, the raw material for the board-scale tests did not provide enough clear wood material for the 30 planned tests per species, and thus not all boards could be tested in all categories, especially for the dry climate of spruce. The relatively small sample size for each category in relation to the variety of the tested material may have limited our ability to investigate some effects according to common evaluation schemes including typical statistical analysis. Thus, alternative evaluation methods in combination with assessment of the experimental results based on MM-model predictions were followed.

The study quantified the influence of different MCs on RS properties by a board-wise evaluation, which yielded similar results for RS stiffness of hardwood on both investigated scales, but not for the RS strength, see Figs. 10 (a)–(d). RS strength on the material scale seems to be hardly influenced by different MCs in contrast to the RS strength on the board scale. As the failure mechanisms on board and material scale are quite similar, they cannot explain the different MC influences. As the number of specimen per climate group are quite small for the large variation of raw material, it is necessary to further investigate on the material scale, if the change in MC has a different influence on the RS stiffness then on the RS strength. Unfortunately, there are to the best of our knowledge no comparable experiments in the literature available.

For beech and birch, the MM-model predicts a minor influence of the annual ring inclination on the RS stiffness of ±10% and a major influence of the density on the RS stiffness of +20% to −50%, for the considered density range, see Figs. 11 (a) and (c). This is in alignment with the experimental results and could explain the observed variation, where the influence of the inclination of the annual rings and density are overlaid. For spruce, the MM-model predicts a reduction of about −75% towards 0° and 90°, which matches well with the experimental results, see Fig. 11 (e). The influence of the density is also given by up to ±50% and closely follows the influence of the annual ring inclination.

No influence of the annual ring inclination on the RS strength becomes obvious in Figs. 11 (b) and (d) for beech and birch. The highest RS strengths of spruce were found around 45° annual ring orientation, while the lowest values were found around 0° and 90°. Thus, there could be a similar trend as for the stiffness, see Fig. 11 (f).

The minor influence of the annual ring orientation on RS properties in hardwood compared to spruce can be explained by their higher density and micro-structural features, e.g. ray cells, reducing the anisotropy in the RT-plane of the material. The influence of additional factors, including annual ring curvature, local densification, and stress non-uniformity, cannot be excluded on the basis of the conducted experiments and modeling. However more detailed assessment of RS behavior would require advanced modeling frameworks that capture cylindrical orthotropic material characteristics and incorporate specimen geometry as well as boundary conditions of the experimental setup, which is beyond the scope of this study.

The RS test setup of the board scale is a modification of the test setup for shear in grain direction of EN 408. The modification includes a change of material in the outer layers and a reduced thickness, but nevertheless investigates effective RS properties of cross-sections including curved annual ring structures, i.e. cylindrical orthotropic behavior. On the contrary, the material-scale tests allow to test rectangular orthotropic behavior. By investigating the effective RS properties on these two characteristic scales, it was possible to identify a major influence of cylindrical orthotropic material behavior on the RS strength of hardwood. The influence on the stiffness was less pronounced, see Fig. 8. As for standardizing RS properties of hardwood, it is of utmost importance to clearly define if cylindrical or rectangular properties are the basis to perform efficient designs for hardwood, especially related to RS strength.

4.5. CPG stiffness and strength

The mean values of the effective compression perpendicular to the grain (CPG) stiffness and strength were calculated for the investigated 18 groups (3 wood species, 2 characteristic scales, 3 ambient climates) and are documented in Table 11. The highest values are identified for the groups conditioned to the dry climate and the lowest values for groups conditioned to the wet climate, except for the stiffness of spruce specimens at the material scale. Further evaluation of the moisture dependence was done in Section 4.6. The CV of the stiffness is higher than the CV of strength compared within one species and scale, except for the birch tests on the material scale.

Comparing CPG stiffness and strength of the different investigated species, a general correlation between a higher stiffness and strength with increased density was confirmed, comparing Tables 2 and 11. Beech had approximately twice the stiffness and strength of birch, and birch had approximately twice the stiffness and strength of spruce. This trend however does not linearly correlate with the mean densities of the 3 different species, as neither beech specimens are twice as dense as birch specimens nor birch specimens are twice as dense as spruce specimens. This correlation between density and CPG stiffness is in agreement with the work of Gibson, Easterling, Ashby and colleagues [23,56,57].

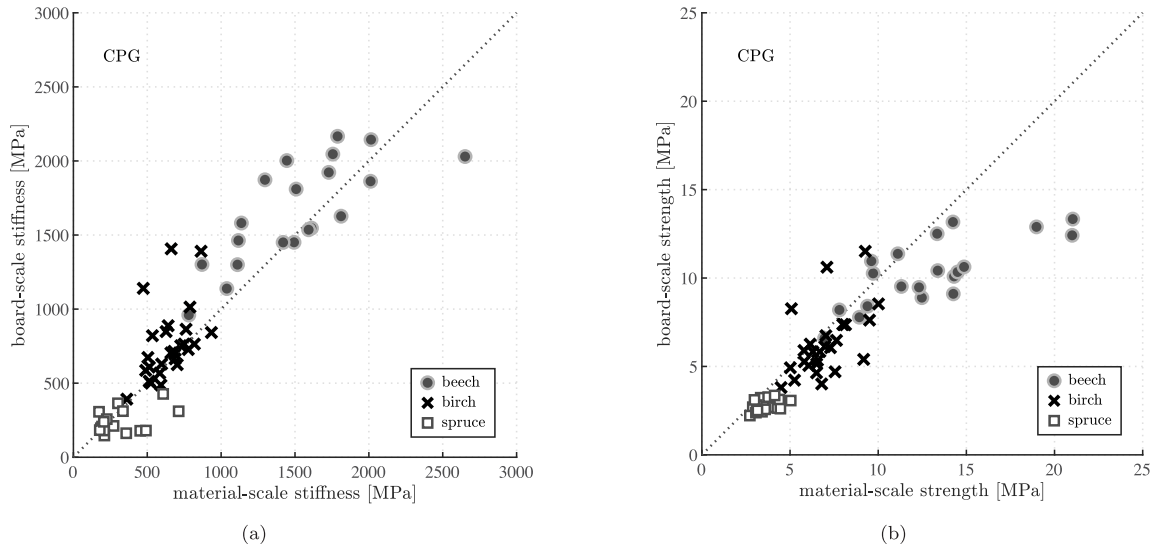

Fig. 12. Correlation plots of CPG (a) stiffness and (b) strength at different scales: individual test results (markers) for beech, birch, and spruce.

The correlation plots of the effective CPG properties at the different investigated scales are presented in Fig. 12. For both hardwood species, the CPG stiffness on the board scale is slightly higher than the stiffness determined on material scale, i.e. 14% higher for beech and 19% higher for birch. CPG stiffness of spruce is 12% lower on the board scale than on the material scale. The board-scale tests led to lower CPG strength values than the material-scale tests for all species, i.e. 17% decrease for beech, 9% decrease for birch, and 22% decrease for spruce. A similar trend of decreasing strength perpendicular to the grain with increasing specimen size was found in [27], however for tension perpendicular to the grain.

Results for CPG stiffness and strength at the standard climate of the three investigated species from literature are listed in Table 12. For the CPG stiffness of beech, the values from literature can be compared to the material-scale tests, where an effective stiffness of 1382 MPa (see Table 11) was found, which is in good agreement with literature data. For birch, the CPG stiffness from literature is about 23% lower than the board-scale result of 807 MPa with a CV of 27% (see Table 11), but would agree well with the stiffness of 629 MPa on the material scale. As regards spruce, comparing literature results for the stiffness with the effective stiffness on the material-scale tests of 297 MPa with a CV of 43.4% (see Table 11) shows that the results were within both ranges, close to the tangential stiffness of Milch et al. [21] and closest to the lowest stiffness at 45° annual ring inclination of Perstorper [30].

As regards the CPG strength of beech, the experimental results presented herein are within the ranges found in literature or slightly higher with 11.3 MPa strength on the material scale, see Table 11. The material-scale results for birch are lower than the range presented by Al-musawi et al. [19]. The results on the board scale agree well with the results from Hübner [47] and Collins and Fink [58], see Table 11. As regards the effective CPG strength of spruce, the range found in literature are higher than the experimental result from the material-scale tests of 4.0 MPa, see Table 11. The comparison of the CPG stiffness and strength with literature does not present a uniform picture, since some experimental results agree well with literature data, while others do not.

The failure modes were similar on board and material scale and the mechanical behavior challenging to characterize, because CPG does not lead to a clearly defined failure mode. For pure radial and tangential loading the specimens get plastic deformed, see Fig. 13(c). The orientation of the annual rings influenced the strength values, with the highest strengths occurring under radial loading. However, in specimens with inclined annual ring orientation, a distinct sliding of annual-ring layers was observed, resulting in a slipping mechanism, see Figs. 13(a) and (d). In beech, a pronounced buckling of the wood rays is locally evident, accompanying the slippage along the annual rings, see Fig. 13(b).

Table 12
CPG experiments in literature performed at standard climate: species, mean density, property (mean stiffness or strength values), corresponding coefficient of variation (CV), and the scale for comparison (board scale (b) or material scale (m)).

CPG Literature reference	species	density [kg/m^3]	property	[MPa]	CV [%]	scale
Milch et al. [21]	beech	–	stiffness	1132–1882	3.7	m
Niemz et al. [22]	beech	–	stiffness	750–1650	–	m
Hübner [47]	beech	–	stiffness	493–2027	27	b
Kollmann & Côté [59]	beech	740	stiffness	1140–2240	–	
Collins & Fink [58]	birch	620	stiffness	620	37	b
Kollmann & Côté [59]	birch	620	stiffness	618–1108	–	
Milch et al. [21]	spruce	–	stiffness	289–362	20	m
Perstorper [30]	spruce	–	stiffness	200–1200	–	m
Kollmann & Côté [59]	spruce	430–500	stiffness	390–890	–	
Al-musawi et al. [19]	beech	594–757	strength	10.8–14.4	–	m
Milch et al. [21]	beech	–	strength	6.4–11.4	–	m
Niemz et al. [22]	beech	–	strength	6–11	–	m
Hübner [47]	beech	–	strength	6.6–12.4	15	b
Al-musawi et al. [19]	birch	561–645	strength	8.1–8.6	–	m
Collins & Fink [58]	birch	620	strength	6.5	28	b
Milch et al. [21]	spruce	–	strength	5.6–6.9	–	m
Kollmann [60]	spruce	–	strength	3.3–3.7	–	m

Table 13
P-values from one-way ANOVA testing the effect of group of 3 ambient climates for conditioning on the response variable (CPG stiffness or CPG strength).

CPG	board scale			material scale		
p-values [-]	beech	birch	spruce	beech	birch	spruce
stiffness	0.1653	0.0410	0.7342	0.1119	0.000003	0.4330
strength	0.0005	0.0031	0.0756	0.0120	0.000052	0.2734

4.6. *Influence of the moisture content on CPG stiffness and strength*

For one third of the investigated properties, the ANOVA yielded no significant influence of the moisture content with p-values larger than 0.05, see Table 13. Considering the results from the multiscale modeling in Fig. 7, the missing significant difference can be ascribed to the more pronounced influence of density in hardwood and annual

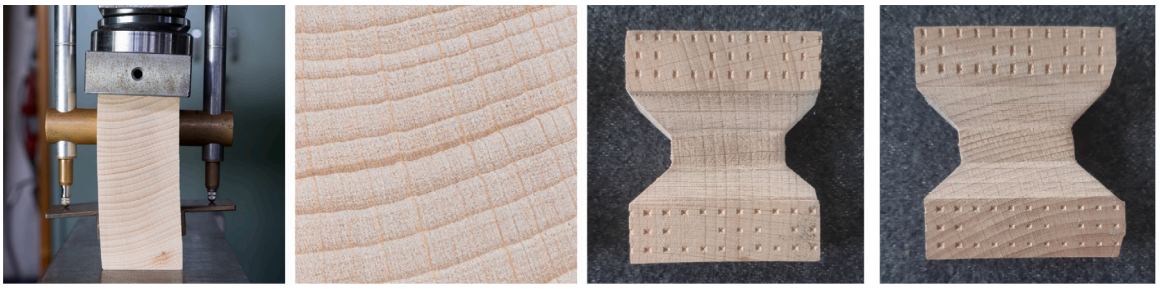

(a) (b) (c) (d)

Fig. 13. CPG specimen with typical plastic deformation: (a) sliding along the annual rings in board-scale specimen; (b) buckling of rays in the sliding process of board-scale specimen; (c) material-scale specimen plastic deformations after tangential loading; (d) sliding along the annual rings in material-scale specimen.

Table 14
Linear moisture content dependence of compression perpendicular to the grain (CPG): change of strength and stiffness per one percent increase of moisture content (k-value) with coefficient of variation (CV) and reference value (RV) at 12% moisture content and relative change compared to the RV [%/%$_{MC}$].

	board scale			material scale		
CPG	beech	birch	spruce	beech	birch	spruce
stiffness k-value [MPa/%$_{MC}$]	−50	−31	−12	−55	−28	−5.6
CV of k-value [%]	58	43	117	80	29	319
RV [MPa]	1594	759	344	1530	647	338
rel. change [%/%$_{MC}$]	3.1	4.1	3.5	3.6	4.3	1.7
strength k-value [MPa/%$_{MC}$]	−0.50	−0.33	−0.097	−0.56	−0.28	−0.065
CV of k-value [%]	34	31	36	42	35	105
RV [MPa]	10.2	6.37	3.05	12.8	7.00	3.98
rel. change [%/%$_{MC}$]	4.9	5.2	3.2	4.4	4.0	1.6

Table 15
MC influence on CPG properties in literature expressed as percent change of the property with 1%-MC change [%/%$_{MC}$]: species, stiffness or strength values (property) and the scale for comparison (board scale (b) or material scale (m)).

CPG Literature reference	species	property	[%/%$_{MC}$]	scale
Niemz et al. [22]	beech	stiffness	5.2–5.5	m
Kollmann [61]	beech	stiffness	1.8–2.5	–
Akter et al. [46]	spruce	stiffness	4.6	m
Brandner [12]	spruce	stiffness	0.5–5.8	b
Kollmann & Côté [59]	Sitka spruce	strength	2.4–3.5	–
Gerhards [62]	var. species	stiffness	2.9–3.3	–
Madsen et al. [63]	var. species	stiffness	3.5–4.3	–
Niemz et al. [22]	beech	strength	4.2–4.8	m
Al-musawi et al. [19]	beech	strength	3.5–4.5	m
Kollmann [61]	beech	strength	4.0	–
Kollmann & Côté [59]	beech	strength	4.0	–
Al-musawi et al. [19]	birch	strength	4.2–6.3	m
Akter et al. [46]	spruce	strength	3.6	m
Brandner [12]	spruce	strength	3.7–4.0	b
Gerhards [62]	var. species	strength	3.8–5.0	–
Madsen et al. [63]	var. species	strength	3.5–4.3	–

ring orientation on stiffness of softwood than differences in MCs. In order to quantify the dependence of the CPG stiffness and strength on the moisture content, the board-wise evaluation method described in Section 3.5 was applied. The average dependencies for the different categories are summarized in Table 14. Both CPG stiffness and strength are shown as a function of the MC in Fig. 14.

Comparison of the MC dependence CPG properties of the three investigated species indicated a stronger MC influence of the CPG properties of hardwood species than spruce.

The CPG stiffness decreases on average by 3.8%/%$_{MC}$ for the hardwood species and 2.6%/%$_{MC}$ for spruce and the CPG strength decreases on average by 4.6%/%$_{MC}$ for the hardwood species and 2.4%/%$_{MC}$ for spruce. The comparison of the scales did not show marked difference in the MC influence between material and board scale. These average values for hardwood are in line with literature, see Table 15 and Fig. 14. The average results for CPG properties of spruce indicate a lower dependency on the MC than literature. A complete comparisons across species, scales, and CPG properties could not be performed, as experimental data was not available in the published literature for some groups, see Table 15.

4.7. Influence of the annual ring inclination on CPG stiffness and strength

As done for RS, an analysis regarding the influence of the orthotropic material properties was conducted in addition while minimizing the dependence of the MC. Fig. 15 shows the normalized (effective) CPG stiffness and strength as a function of the annual ring inclination of the material-scale specimens and the corresponding mean properties at the board scale, trend lines from the CPG stiffness predicted by the MM-model, as well as property ranges from literature listed in Table 12.

The CPG stiffness of beech is influenced by the annual ring inclination and shows an increase of up to +50% at around 0°, which is related to loading in the radial direction, and a corresponding decrease towards 90° (tangential direction), see Fig. 15 (a). The experimental findings of CPG stiffness of birch however did not show such a dependence on the annual ring inclination, see Fig. 15 (c). The experimental results of CPG stiffness of spruce showed a clear dependence on the annual ring inclination, with a peak around 0° (radial direction), a minimum at around 45°, and an increase towards 90° (tangential direction), see Fig. 15 (e).

Comparing the MM-model with the CPG stiffness on the material scale, the predictions show good agreement for beech and spruce, but not for birch, as the MM-model would predict a strong dependence on the annual ring inclination, but the experimental results did not show this dependence. For spruce, the MM-model predictions and the experimental results agree quite well although the results of the model are shifted to slightly higher relative values than the experiments.

The experimentally measured CPG strengths of beech indicate an influence on the annual ring inclination. The strength showed a peak at an annual ring inclination of around 0° (radial direction), a decrease towards 45° and similar values at around 90°, see Fig. 15 (b). The strength of birch was not influenced by the inclination of the annual rings, see Fig. 15 (d). For the CPG strength of spruce, a slight increase towards 0° and 90° with lower values at around 45° could be indicated from the experiments, see Fig. 15 (f).

Milch et al. [21] found about 65% and 78% higher values in the CPG stiffness and strength of beech in radial direction than in tangential direction. These results agree quite well with the distribution

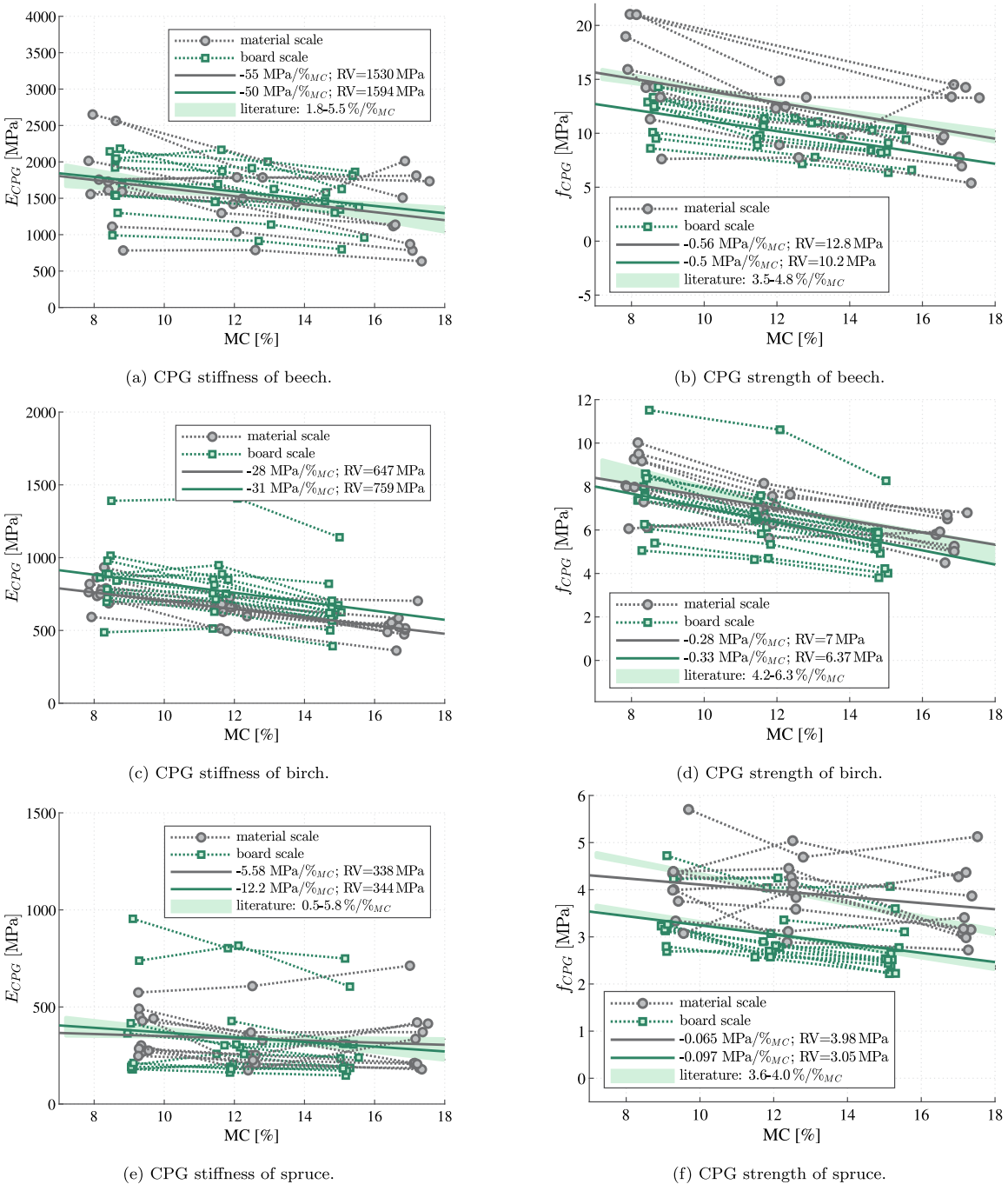

(a) CPG stiffness of beech.

(b) CPG strength of beech.

(c) CPG stiffness of birch.

(d) CPG strength of birch.

(e) CPG stiffness of spruce.

(f) CPG strength of spruce.

Fig. 14. Experimental results for CPG stiffness E_{CPG} and CPG strength f_{CPG}: individual test results (markers), board results (dotted lines between markers), and average group fit for board and material scales (continuous lines); available literature values for comparison listed in Table 15 evaluated for the RV of the conducted experiments (shaded area).

of stiffness and strength over the annual ring inclination of beech in Figs. 15(a) and (b). Furthermore, Al-musawi et al. [64] found higher CPG stiffness and strength of beech and birch in radial direction than in tangential direction. They assumed a stronger influence of the orientation of the rays than the annual ring inclination itself, where annual ring inclination and rays are linked to each other. The material-scale results of CPG stiffness and strength of beech (Figs. 15(a) and (b)) agree well with the previous findings.

The experimental results of birch do not agree with the results from Al-musawi et al. [64] (Figs. 15(c) and (d)), as there was no clear correlation between annual ring inclination and CPG stiffness and strength. On the other hand, the MM-modeling and the results from Collins and Fink [58] agree well with Al-musawi et al. [64]. Therefore, the influence of the annual ring inclination might have been masked by density variety of the birch samples. Collins and Fink [58] found a significant correlation between the annual ring inclination and the CPG stiffness but less correlation to CPG strength, with higher values for radially loaded boards than for tangentially loaded boards.

For CPG stiffness and strength of spruce, Milch et al. [21] found 25% higher stiffness and 19% lower strength in radial direction than in tangential direction. Perstorper [30] found the lowest CPG strength at around 45° annual ring inclination and the highest close to 0° (radial direction), which were about 6 times larger. The CPG stiffness in tangential direction was a bit smaller than in radial direction and

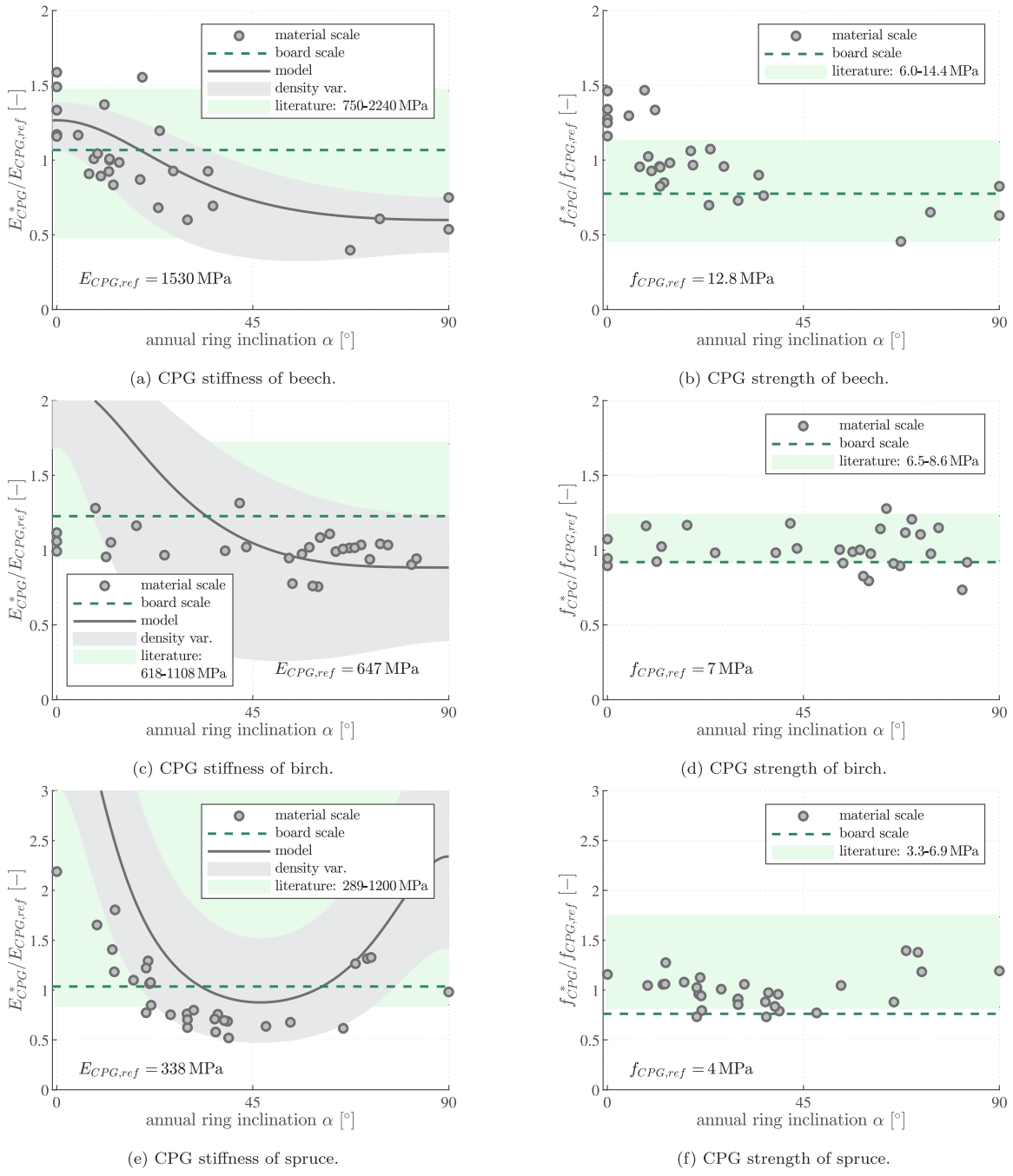

(a) CPG stiffness of beech.

(b) CPG strength of beech.

(c) CPG stiffness of birch.

(d) CPG strength of birch.

(e) CPG stiffness of spruce.

(f) CPG strength of spruce.

Fig. 15. Influence of annual ring inclination on normalized CPG stiffness $E^*_{CPG}/E_{CPG,ref}$ and normalized CPG strength $f^*_{CPG}/f_{CPG,ref}$: individual test results on the material scale (markers), results on the board scale from Table 7 (dashed green line — mean value standard climate), model prediction (continuous line — mean value standard climate; light gray shaded area — density variation between upper and lower density), and strength and stiffness range from literature listed in Table 12 (light green shaded area).

about 4 to 5 times larger than the smallest values. These earlier findings cannot be directly confirmed with the experimental results at the material scale, see Figs. 15(e) and (f). The test series on the material scale of spruce hardly included specimens with 0° (radial direction) and 90° (tangential direction) annual ring inclination and the MM-modeling indicates a strong dependence on the annual ring inclination with a minimum around 45° annual ring inclination, as well as a slightly higher stiffness in radial direction than in tangential direction. This is in agreement with the results of Perstorper [30] and Milch et al. [21] for the CPG stiffness.

Overall, the influence of the annual ring inclination and sawing pattern on the CPG properties were hardly investigated in literature, but a minimum of one experimental dataset could be found for comparison for all groups of different species and mechanical properties.

4.8. Further aspects of the CPG stiffness and strength investigation

The measuring length of the experimental setup for the board-scale tests was 54 mm and the thickness perpendicular to the measuring length was 40 mm, see Fig. 2. This area could be considered too small

to investigate cylindrical orthotropic material behavior of timber, especially for specimens cut from outer parts of the trunk. In comparison to the investigated area of the material-scale specimens (10 mm×30 mm), the area in the board-test specimens is about seven times larger and the aspect ratio is different and thus the cylindrical aspect is much more present. The differences in effective parameters between the investigated scales are moderate, but clearly show that for testing CPG properties it is important to distinguish cylindrical and rectangular orthotropic material behavior. Especially when the effective properties are used for engineering design.

The investigation of the annual ring inclination on the CPG properties on the material scale yielded an influence on the properties of beech and spruce, but not on the CPG stiffness and strength of birch, see Fig. 15. The applied evaluation method considered different MC content, but not different densities and thus the results of birch were reevaluated by normalizing the properties by the individual densities. This second evaluation showed that the density was masking the influence of the annual ring inclination, which was quite similar to the influence on the beech samples. Why the influence of the annual ring inclination was masked by the density for birch but not for beech might be explained from the MM-model predictions in Figs. 15(a) and (c). For birch the influence of the density variation is larger than for beech, and also the influence of the annual ring orientation was predicted larger. The density influence could be more pronounced due to the more uniform micro-structure of birch than of beech or the combination of densities and annual rings orientations of the specimens.

5. Conclusions

This work summarizes an extensive experimental investigation of stiffness and strength in rolling shear (RS) and compression perpendicular to grain (CPG) of beech, birch, and spruce. The testing campaign included different ambient climates representative for climate classes 1 and 2, and two different characteristic length scales to investigate the influence of the annual ring structure. To capture a large variety of each wood species, the investigated 11 boards of beech had densities from 661 to 821 kg/m^3, the 13 boards of birch had densities from 541 to 718 kg/m^3, and the 13 boards of spruce had densities from 426 to 480 kg/m^3. This large variety from the investigated material yielded low statistical significance of the investigated groups and thus a board-wise quantification was applied and further insights were drawn from comparison with micromechanical models. The following conclusions can be drawn from this experimental study regarding the influence of the applied test method, the moisture content, and annual ring structure.

- The testing methods and corresponding sizes of the test specimens had a major influence on the RS strength. The cylindrical orthotropic behavior of the larger board specimens increased the RS strength of beech and birch by 80% compared to the smaller specimens. This underlines the utmost importance of mechanical models that can describe this relationship for application in engineering design.
- An overall MC influence of 3%/%$_{MC}$ on RS stiffness and strength parameter of all species with a quite wide range of dispersion can be concluded. For the MC dependence of the CPG parameters, a distinction between hardwood and spruce is possible. Hardwood CPG properties were influenced more strongly with 3.8 and 4.6%/%$_{MC}$ for stiffness and strength than spruce stiffness and strength with 2.6 and 2.4%/%$_{MC}$.
- For the RS stiffness and strength on the material scale of beech and birch, there was hardly any dependence on the annual ring inclination. For spruce, a clear dependence of the RS stiffness and strength on the annual ring inclination became obvious from the experimental results. CPG stiffness and strength of beech and spruce showed a dependence on the annual ring inclination with highest values close to 0° annual ring inclination (loading in radial direction), whereas for birch, no influence was obvious from the experimental results, but probably masked by density variations.
- The micromechanical modeling confirmed that the annual ring inclination has a considerably smaller influence on the RS stiffness of beech and birch as compared to spruce. The modeling showed a major influence of the density of hardwood on the RS stiffness. For CPG stiffness the model predicted a dependence on the annual ring inclination for all wood species, which agreed qualitatively very well with the experimental results of beech and spruce.
- Comparisons of the experimental results with previous works revealed partly contradicting findings and a lack of experimental data especially for the dependence of the CPG properties of different wood species on the annual ring inclination.
- Experimental investigations on the influence of MC are challenging as mechanical properties of wood are influenced also by many factors among others density and orthotropic material behavior. Evaluating the influence on specimens from the same board is beneficial to quantify the influence for a group of specimens with a low statistical significance. Keeping a good balance between uniform material and variety is essential.

The broad variability of the investigated material likely reduced the sensitivity of conventional statistical analyses and limited the identification of significant individual effects. However, trends observed across experimental configurations and supported by modeling suggest that the derived conclusions are robust, although further studies with more controlled material selection and sampling are beneficial for more detailed quantification in the future.

CRediT authorship contribution statement

Eva Binder: Writing – review & editing, Writing – original draft, Visualization, Supervision, Software, Project administration, Methodology, Investigation, Formal analysis, Data curation, Conceptualization. **Elisabet Kuck:** Writing – review & editing, Writing – original draft, Software, Methodology, Investigation, Formal analysis, Data curation. **Christian Bertram:** Writing – review & editing, Writing – original draft, Software, Methodology, Investigation, Formal analysis, Data curation. **Zijad Shehadeh:** Writing – review & editing, Software, Investigation, Data curation. **Michael Schweigler:** Writing – review & editing, Validation, Methodology. **Carmen Sandhaas:** Writing – review & editing, Validation, Supervision, Project administration, Methodology, Conceptualization. **Thomas K. Bader:** Writing – review & editing, Writing – original draft, Validation, Supervision, Project administration, Methodology, Funding acquisition, Conceptualization.

Funding

This work was supported by the Södra Foundation for Research, Development and Education under the project "Moisture and time dependent properties of southern Swedish hardwood for load bearing structures". In addition, Eva Binder gratefully acknowledges the financial support provided by the KK Knowledge Foundation within the proposal 'Biträdande lektor i hybrid och samverkanskonstruktioner' granted to Linnaeus University in the call 2021 [grant number 2021007001H].

Declaration of competing interest

The authors declare that they have no known competing financial interests or personal relationships that could have appeared to influence the work reported in this paper.

Acknowledgments

Special thanks to Daniel Gustafsson and Anders Alrutz from Linnaeus University and the laboratory staff from the Research Center for Steel, Timber and Masonry at Karlsruhe Institute of Technology for their invaluable assistance with the preparation of specimens and experimental setups in the laboratory. Their support and expertise were crucial to the successful completion of this work.

Data availability

Data will be made available on request.

References

[1] Intergovernmental Panel on Climate Change, in: J.S. Priyadarshi R. Shukla (Ed.), Climate Change 2022 - Mitigation of Climate Change: Working Group III Contribution to the Sixth Assessment Report of the Intergovernmental Panel on Climate Change, Cambridge University Press, 2023, http://dx.doi.org/10.1017/9781009157926.

[2] M. Erdozain, I. Alberdi, R. Aszalós, K. Bollmann, V. Detsis, J. Diaci, M. Đodan, G. Efthimiou, L. Gálhidy, M. Haase, J. Hoffmann, D. Jaymond, E. Johann, H. Jørgensen, F. Krumm, T. Kuuluvainen, T. Lachat, K. Lapin, M. Lindner, P. Madsen, L. Nichiforel, M. Pach, Y. Paillet, C. Palaghianu, J. Palau, J. Pemán, S. Perić, S. Raum, S. Schueler, J. Skrzyszewski, J. Svensson, S. Teeuwen, G. Vacchiano, K. Vandekerkhove, I. Cañellas, M. Menéndez-Miguélez, L.L.K. Werden, A. Àvila, S. de Miguel, The evolution of forest restoration in Europe: A synthesis for a step forward based on national expert knowledge, Curr. For. Rep. 11 (1) (2024) http://dx.doi.org/10.1007/s40725-024-00235-3.

[3] S. Neuner, A. Albrecht, D. Cullmann, F. Engels, V.C. Griess, W.A. Hahn, M. Hanewinkel, F. Härtl, C. Kölling, K. Staupendahl, T. Knoke, Survival of Norway spruce remains higher in mixed stands under a dryer and warmer climate, Global Change Biol. 21 (2) (2014) 935–946, http://dx.doi.org/10.1111/gcb.12751.

[4] T. Hiura, S. Go, H. Iijima, Long-term forest dynamics in response to climate change in northern mixed forests in Japan: A 38-year individual-based approach, Forest Ecol. Manag. 449 (2019) 117469, http://dx.doi.org/10.1016/j.foreco.2019.117469.

[5] D. Lee, E. Holmström, J. Hynynen, U. Nilsson, K.T. Korhonen, B. Westerlund, S. Bianchi, J. Aldea, S. Huuskonen, Current state of mixed forests available for wood supply in Finland and Sweden, Scand. J. For. Res. 38 (7–8) (2023) 442–452, http://dx.doi.org/10.1080/02827581.2023.2259797.

[6] H. Petersson, Skogsdata 2024, SLU Institutionen för skoglig resurshushållning, 2024.

[7] Forest Statistics 2024 - Official Statistics of Sweden, Swedish University of Agricultural Sciences, 2024.

[8] L. Woxblom, M. Nylinder, Broadleaved Forests in southern Sweden: Management for multiple goals, Ecol. Bull. 53 (2010) 43–50.

[9] A. Olsson, W. Schirén, M. Hu, Dynamic and quasi-static evaluation of stiffness properties of CLT: longitudinal MoE and effective rolling shear modulus, Eur. J. Wood Wood Prod. 83 (1) (2024) http://dx.doi.org/10.1007/s00107-024-02185-w.

[10] M. Li, Evaluating rolling shear strength properties of cross-laminated timber by short-span bending tests and modified planar shear tests, J. Wood Sci. 63 (4) (2017) 331–337, http://dx.doi.org/10.1007/s10086-017-1631-6.

[11] D. Glasner, A. Ringhofer, R. Brandner, G. Schickhofer, Rolling shear strength of cross laminated timber (CLT)—Testing, evaluation, and design, Buildings 13 (11) (2023) 2831, http://dx.doi.org/10.3390/buildings13112831.

[12] R. Brandner, Cross laminated timber (CLT) in compression perpendicular to plane: Testing, properties, design and recommendations for harmonizing design provisions for structural timber products, Eng. Struct. 171 (2018) 944–960, http://dx.doi.org/10.1016/j.engstruct.2018.02.076.

[13] T. Ehrhart, R. Brandner, Rolling shear: Test configurations and properties of some European soft- and hardwood species, Eng. Struct. 172 (2018) 554–572, http://dx.doi.org/10.1016/j.engstruct.2018.05.118.

[14] D.P. Pasca, F.M. Massaro, Y. De Santis, H. Stamatopoulos, J. Ljungdahl, A. Aloisio, Deformation level and specimen geometry in compression perpendicular to the grain of solid timber, GLT and CLT timber products, Eng. Struct. 321 (2024) 118972, http://dx.doi.org/10.1016/j.engstruct.2024.118972.

[15] S. Aicher, M. Hirsch, Z. Christian, Hybrid cross-laminated timber plates with beech wood cross-layers, Constr. Build. Mater. 124 (2016) 1007–1018, http://dx.doi.org/10.1016/j.conbuildmat.2016.08.051.

[16] A. Muraleedharan, S. Markus Reiterer, Combined glued laminated timber using hardwood and softwood lamellas (Master's thesis), Linnaeus University, Department of Building Technology, 2016.

[17] S. Glass, S. Zelinka, in: W. Madison (Ed.), Wood Handbook - Wood as an Engineering Material. General Technical Report FPL-GTR-282, U.S. Department of Agriculture, Forest Service, Forest Products Laboratory, 2021, p. 22.

[18] P. Niemz, W. Sonderegger, G. Gorbacheva, Springer handbook of wood science and technology., in: P. Niemz, A. Teischinger, D. Sandberg (Eds.), Springer Handbook of Wood Science and Technology, Springer International Publishing, 2023, pp. 399–439, http://dx.doi.org/10.1007/978-3-030-81315-4_8.

[19] H. Al-musawi, C. Huber, M. Grabner, B. Ungerer, T. Krenke, P. Matz, A. Teischinger, U. Müller, Compressive strength of beech and birch at different moisture contents and temperatures, J. Mater. Sci. 58 (35) (2023) 13994–14008, http://dx.doi.org/10.1007/s10853-023-08882-w.

[20] V. Borůvka, D. Novák, P. Šedivka, Comparison and analysis of radial and tangential bending of softwood and hardwood at static and dynamic loading, Forests 11 (8) (2020) 896, http://dx.doi.org/10.3390/f11080896.

[21] J. Milch, J. Tippner, V. Sebera, M. Brabec, Determination of the elasto-plastic material characteristics of Norway spruce and European beech wood by experimental and numerical analyses, Holzforschung 70 (11) (2016) 1081–1092, http://dx.doi.org/10.1515/hf-2015-0267.

[22] P. Niemz, T. Ozyhar, S. Hering, W. Sonderegger, Zur Orthotropie der physikalisch-mechanischen Eigenschaften von Rotbuchenholz, Bautechnik 92 (1) (2015) 3–8, http://dx.doi.org/10.1002/bate.201400079.

[23] L.J. Gibson, The hierarchical structure and mechanics of plant materials, J. R. Soc. Interface 9 (76) (2012) 2749–2766, http://dx.doi.org/10.1098/rsif.2012.0341.

[24] S. Aicher, G. Dill-Langer, Basic considerations to rolling shear modulus in wooden boards, Otto-Graf-Journal 11 (2000) 157.

[25] S. Clauß, C. Pescatore, P. Niemz, Anisotropic elastic properties of common ash (Fraxinus excelsior L.), Holzforschung 68 (8) (2014) 941–949, http://dx.doi.org/10.1515/hf-2013-0189.

[26] M. Aydın, T.Y. Aydın, Influence of growth ring number and width on elastic constants of poplar, BioResources 18 (4) (2023) 8484–8502, http://dx.doi.org/10.15376/biores.18.4.8484-8502.

[27] M.U. Pedersen, C.O. Clorius, L. Damkilde, P. Hoffmeyer, A simple size effect model for tension perpendicular to the grain, Wood Sci. Technol. 37 (2) (2003) 125–140, http://dx.doi.org/10.1007/s00226-003-0168-6.

[28] P. Niemz, W. Sonderegger, P.J. Gustafsson, B. Kasal, T. Polocoşer, Springer handbook of wood science and technology., in: P. Niemz, A. Teischinger, D. Sandberg (Eds.), Springer Handbook of Wood Science and Technology, Springer International Publishing, 2023, pp. 441–505, http://dx.doi.org/10.1007/978-3-030-81315-4_8.

[29] S.T. Akter, T.K. Bader, Experimental assessment of failure criteria for the interaction of normal stress perpendicular to the grain with rolling shear stress in Norway spruce clear wood, Eur. J. Wood Wood Prod. 78 (6) (2020) 1105–1123, http://dx.doi.org/10.1007/s00107-020-01587-w.

[30] M. Perstorper, Dynamic test for determination of rolling shear modulus of wood, in: J.S. Gomes (Ed.), Proceedings ICEM20 - Experimental Mechanics in Engineering and Biomechanics, 2023.

[31] T.K. Bader, K. Hofstetter, C. Hellmich, J. Eberhardsteiner, The poroelastic role of water in cell walls of the hierarchical composite "softwood", Acta Mech. 217 (1–2) (2010) 75–100, http://dx.doi.org/10.1007/s00707-010-0368-8.

[32] K. de Borst, T. Bader, Structure–function relationships in hardwood – insight from micromechanical modelling, J. Theoret. Biol. 345 (2014) 78–91, http://dx.doi.org/10.1016/j.jtbi.2013.12.013.

[33] H.J. Blaß, C. Sandhaas, Timber Engineering-Principles for Design, KIT Scientific Publishing, 2017.

[34] R. Wagenführ, Holzatlas, in: A. Wagenführ (Ed.), 7., überarbeitete und ergänzte Auflage, in: Hanser eLibrary, Hanser, München, 2022.

[35] T. Ehrhart, R. Steiger, P. Palma, A. Frangi, Estimation of the tensile strength of European beech timber boards based on density, dynamic modulus of elasticity and local fibre orienation, 2018, http://dx.doi.org/10.3929/ETHZ-B-000286967.

[36] E. Guntekin, S. Ozkan, T. Yilmaz, Prediction of bending properties for beech lumber using stress wave method, Maderas. Cienc. Y Tecnología 16 (1) (2014) 93–98, http://dx.doi.org/10.4067/s0718-221x2014005000008.

[37] A. Rais, J.-W.G. van de Kuilen, H. Pretzsch, Impact of species mixture on the stiffness of European beech (Fagus sylvatica L.) sawn timber, Forest Ecol. Manag. 461 (2020) 117935, http://dx.doi.org/10.1016/j.foreco.2020.117935.

[38] M. Johansson, H. Säll, S.-O. Lundqvist, Properties of Materials from Birch–Variations and Relationships: Part 2. Mechanical and Physical Properties, Linnaeus University, 2013.

[39] F.F. Kollmann, E.W. Kuenzi, A.J. Stamm, Principles of Wood Science and Technology: II Wood Based Materials, Springer Science & Business Media, 2012.

[40] European Committee for Standardization, EN408:2010+A1:2012: Timber structures - Structural timber and glued laminated timber- Determination of some physical and mechanical properties,

[41] P. Mestek, Punktgestützte Flächentragwerke aus Brettsperrholz (BSP)–Schubbemessung unter Berücksichtigung von Schubverstärkungen (Ph.D. thesis), Technische Universität München, 2011.

[42] R. Nero, P. Christopher, T. Ngo, Investigation of rolling shear properties of cross-laminated timber (CLT) and comparison of experimental approaches, Constr. Build. Mater. 316 (2022) 125897, http://dx.doi.org/10.1016/j.conbuildmat.2021.125897.

[43] S. Collins, G. Fink, Experimental investigation on the rolling shaer properties of timber, in: World Conference on Timber Engineering 2025, in: WCTE 2025, World Conference On Timber Engineering 2025, 2025, pp. 2169–2174, http://dx.doi.org/10.52202/080513-0265.
[44] European Committee for Standardization, EN1995-1-1:2004 Eurocode 5: Design of timber structures - Part 1-1: General - Common rules and rules for buildings, Swedish standards institute (SIS), 2004.
[45] European Committee for Standardization, EN13183-1:2004: Moisture content of a piece of sawn timber - Part 1: Determination by oven dry method.
[46] S.T. Akter, E. Binder, T.K. Bader, Moisture and short-term time-dependent behavior of Norway spruce clear wood under compression perpendicular to the grain and rolling shear, Wood Mater. Sci. Eng. 18 (2) (2022) 580–593, http://dx.doi.org/10.1080/17480272.2022.2056715.
[47] U. Hübner, in: G. Schickhofer, H.J. Blaß, E. Gehri (Eds.), Mechanische Kengrößen von Buchen-, Eschen- und Robinienholz für lastabtragende Bauteile, Verlag der Technischen Universität, Graz, 2013.
[48] T.M. Inc., Matlab R2022b, 2022, URL https://www.mathworks.com.
[49] K. Hofstetter, C. Hellmich, J. Eberhardsteiner, Development and experimental validation of a continuum micromechanics model for the elasticity of wood, Eur. J. Mech. A Solids 24 (6) (2005) 1030–1053, http://dx.doi.org/10.1016/j.euromechsol.2005.05.006.
[50] S. Aicher, Z. Christian, M. Hirsch, Rolling shear modulus and strength of beech wood laminations, Holzforschung 70 (8) (2016) 773–781, http://dx.doi.org/10.1515/hf-2015-0229.
[51] F.H. Neuhaus, Elastizitätszahlen von Fichtenholz in Abhängigkeit von der Holzfeuchtigkeit, Ruhr-Universität Bochum, Institut für Konstruktiven Ingenieurbau, 1981.
[52] R. Görlacher, Ein Verfahren zur Ermittlung des Rollschubmoduls von Holz, Holz als Roh- und Werkst. 60 (5) (2002) 317–322, http://dx.doi.org/10.1007/s00107-002-0317-x.
[53] B. Hassel, P. Berard, C. Modén, L. Berglund, The single cube apparatus for shear testing – full-field strain data and finite element analysis of wood in transverse shear, Compos. Sci. Technol. 69 (7–8) (2009) 877–882, http://dx.doi.org/10.1016/j.compscitech.2008.11.013.
[54] M. Flaig, Biegeträger aus Brettsperrholz bei Beanspruchung in Plattenebene, vol. 26, KIT Scientific Publishing, 2014.
[55] X. Sun, M. He, Z. Li, Experimental investigation on the influence of lamination aspect ratios on rolling shear strength of cross-laminated timber, Arch. Civ. Mech. Eng. 22 (1) (2021) http://dx.doi.org/10.1007/s43452-021-00345-w.
[56] K.E. Easterling, R. Harrysson, L.J. Gibson, M.F. Ashby, On the mechanics of balsa and other woods, Proc. R. Soc. Lond. Ser. A, Math. Phys. Sci. 383 (1784) (1982) 31–41.
[57] M.F. Ashby, L.J. Gibson, Cellular solids: Structure and properties, Press Syndicate of the University of Cambridge, Cambridge, UK, 1997, pp. 175–231.
[58] S. Collins, G. Fink, Mechanical behaviour of sawn timber of silver birch under compression loading, Wood Mater. Sci. & Eng. 17 (2) (2020) 121–128, http://dx.doi.org/10.1080/17480272.2020.1801836.
[59] F.F.P. Kollmann, W.A. Côté, Principles of Wood Science and Technology: I Solid Wood, Springer Berlin Heidelberg, 1968, http://dx.doi.org/10.1007/978-3-642-87928-9.
[60] F. Kollmann, Kollmann, 2., neubearb. u. erw. Aufl. 1951, Repr., in: Technologie des Holzes und der Holzwerkstoffe, vol. 1, (1 (1,2,1982)) Springer, Berlin, 1982.
[61] F. Kollmann, Zur Frage der Querdruckfestigkeit von Holz, Holzforsch. und Holzverwert. 11 (5) (1959) 109–121.
[62] C.C. Gerhards, Effect of moisture content and temperature on the mechanical properties of wood: An analysis of immediate effects, Wood Fiber Sci. (1982) 4–36.
[63] B. Madsen, R. Hooley, C. Hall, A design method for bearing stresses in wood, Can. J. Civ. Eng. 9 (2) (1982) 338–349.
[64] H. Al-musawi, C. Huber, B. Ungerer, M. Jakob, M. Pramreiter, P. Halbauer, J. Painer, T. Krenke, U. Müller, The effect of rays on the mechanical behaviour of beech and birch at different moisture and temperature conditions perpendicular to the grain, Forests 15 (4) (2024) 584, http://dx.doi.org/10.3390/f15040584.